Analysis of Reactor Simulations Using Surrogate Models

Thesis Defense

Artem Yankov

University of Michigan

December 8, 2014

Outline

Background

- Physical phenomena is studied by conducting experiments.
- Any data collected represents instances of underlying stochastic processes.
- We build predictive computer models in an attempt to reproduce such observed physical phenomena.
- To accurately capture stochastic element of experiments, computer models should be probabilistic.
- In other words, inputs to computer models have uncertainties associated with them that are propagated to any outputs of interest.
- Running computer simulations should be like conducting physical experiments. Computer experiments.

Why Surrogates?

- We run computer simulations to meet design objectives under certain constraints.
- Involves numerical optimization, calibration, and performing what-if analyses.
- Also, we're interested in determining which of our design variables have the greatest effects on simulation outcomes.
- Thousands of simulations required to make this possible but...
- Computer simulations that model real phenomenon like nuclear reactors often take $\mathcal{O}(\text{hours})$ or $\mathcal{O}(\text{days})$ to complete.
- Building a surrogate model for your expensive computer simulations can make everything listed above possible.

What is a Surrogate Model?

- A model for the outcomes of (likely) expensive computer simulations that can be rapidly evaluated while simultaneously preserving the predictive capabilities of the original simulations.
- Want to intelligently choose subspace $\{x_1, x_2, ..., x_N\} \subset \mathbf{X}$ to sample expensive computer code to get $\{y_1, y_2, ..., y_N\} \subset \mathbf{Y}$.
- Learn fast mapping that approximates $\mathbf{X} \rightarrow \mathbf{Y}$.

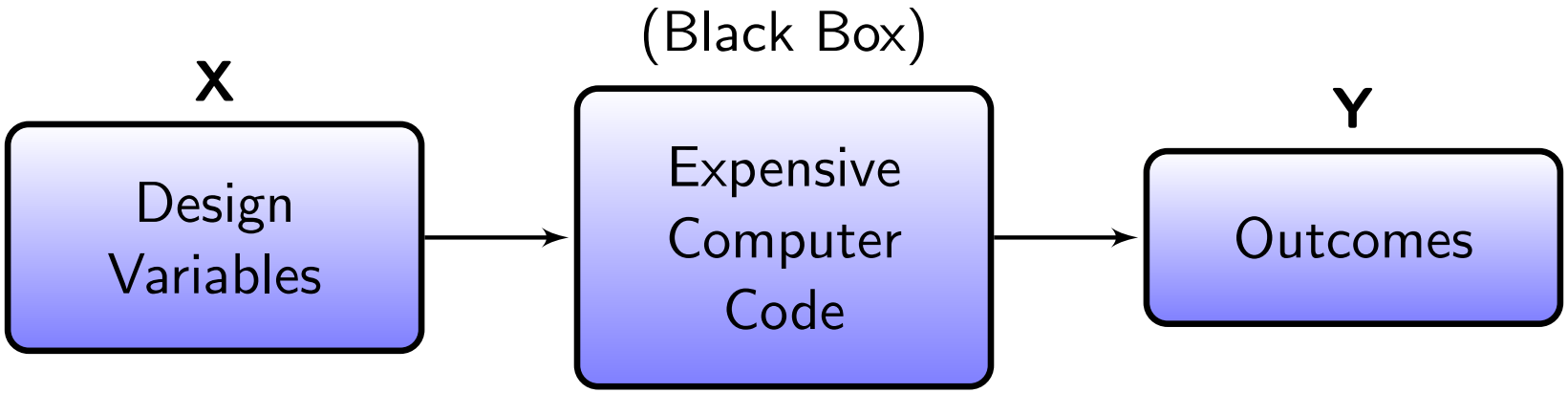

Proposed Application to Fuel Performance Modeling

- Fission Gas Release (FGR) refers to the phenomenon where Xenon and Krypton gases formed in UO_2 fuel rods are released into the rod filling gas.
- Causes pressure build-up and thermal conductivity degradation in the rod filling gas, potentially jeopardizing the safety of the reactor.
- Fission gas atoms generated in the fuel grains diffuse towards the grain boundaries.
- Majority of the gas diffuses into grain-face gas bubbles, giving rise to grain-face swelling.
- Bubble growth brings about bubble coalescence and interconnection, eventually leading to the formation of a tunnel network through which the fission gas is released.

SIFGRS FGR Model

- Simple Integrated Fission Gas Release and Swelling (SIFGRS)
- Incorporates gas diffusion and precipitation in grains, growth and coalescence of gas bubbles at grain faces, thermal, athermal, steady-state, and transient gas release.
- Through a direct description of the grain face gas bubble development, the fission gas swelling and release are calculated as coupled processes.
- Parameterized by, among others, linear heat rate, gas diffusion coefficient, surface tension of grain face bubbles, hydrostatic pressure, fuel grain radius, fuel porosity, and grain boundary sweeping.

Risø AN3 Experiment

- Validation case for fuel performance modeling in the Fumex-II database.
- Experiment consists of a base irradiation of four reactor cycles in the Biblis A pressurized water reactor.
- After the base irradiation period, a fuel rod is extracted and refabricated to a shorter length before undergoing a power ramp.
- Refabricated fuel rod is outfitted with various instrumentation such that fuel centerline temperature, FGR and rod internal pressure measurements can be obtained.

Risø AN3 Experiment Irradiation Profiles

Base Irradiation History

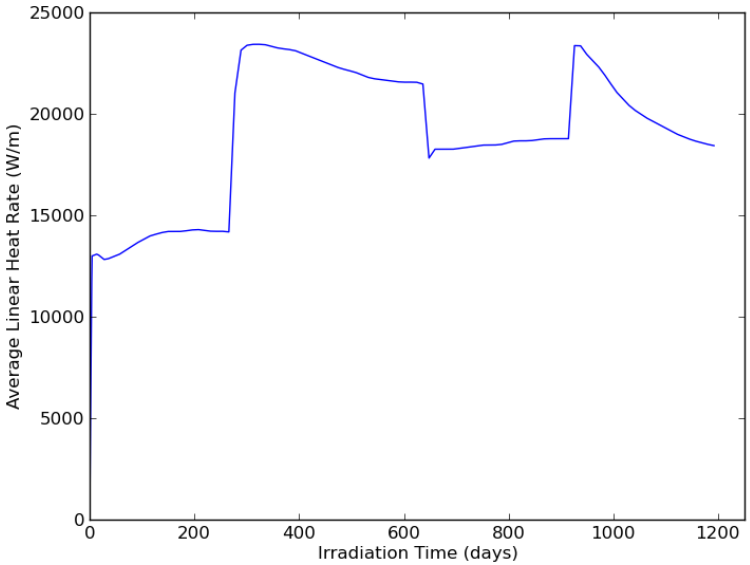

Power Ramp Experiment

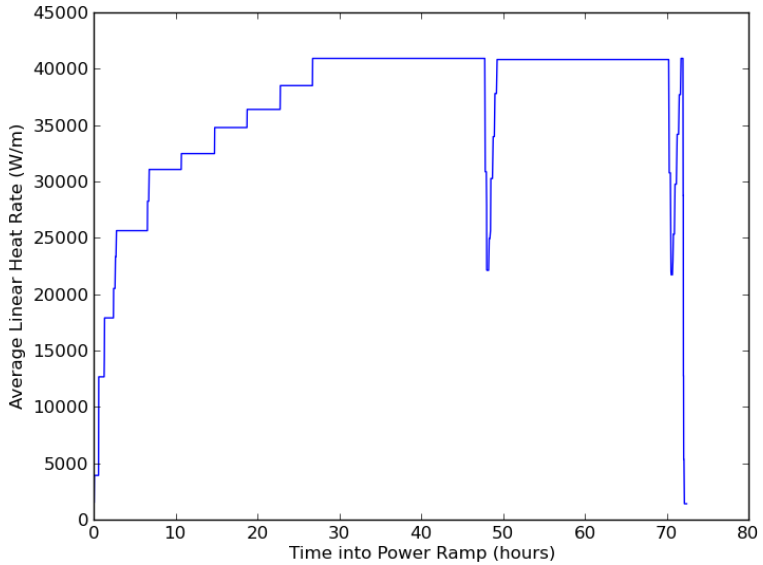

Modeling Risø AN3 Experiment with Bison

- Bison is a finite-element fuel performance modeling code that utilizes the SIFGRS model.
- SIFGRS parameters are quite generic and uncertain.

Fission Gas Release

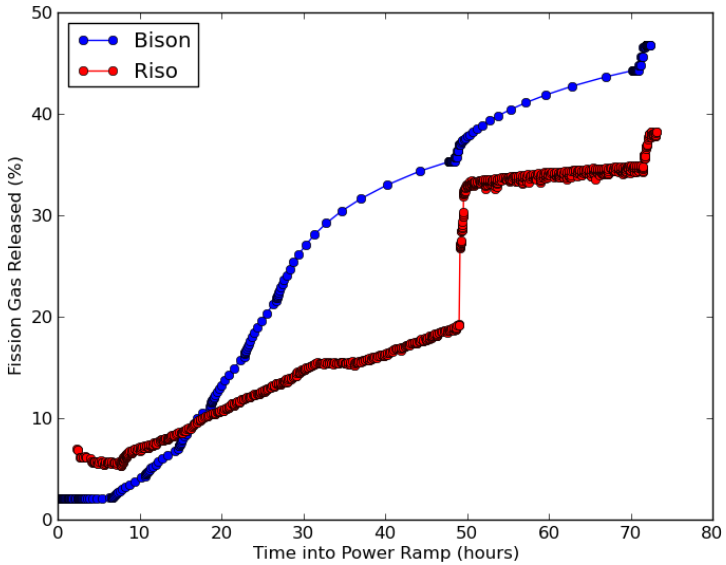

Fuel Centerline Temperature

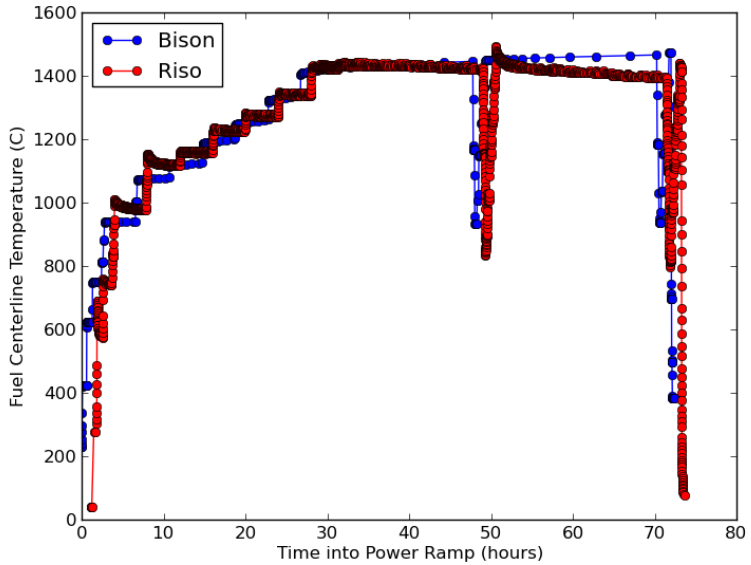

Modeling Risø AN3 Experiment with Bison

- Bison predictions of FGR and temperature fields stand to be improved by calibrating FGR parameters to experimental data.
- Calibration studies require $\mathcal{O}(10^3)$ function evaluations, which in this is the Bison computer code.
- Each simulation of the Risø AN3 experiment will take a few hours on multiple processors.
- It's necessary to construct a surrogate for the calibration study.

Outline

Classic Overview

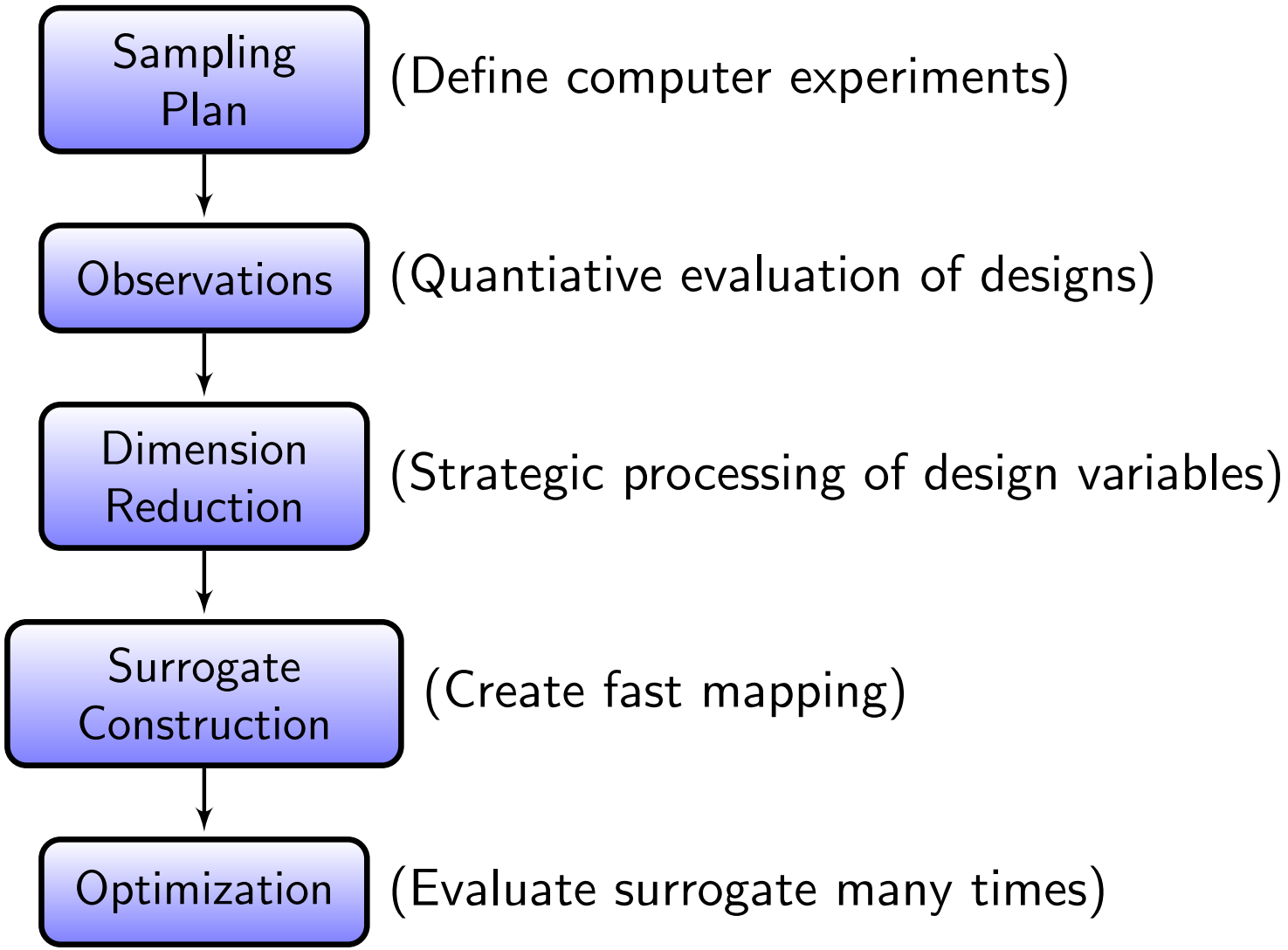

Kriging vs. anchored-ANOVA Collocation

Kriging

- Dimension reduction processed separately
- Sampling points random
- User determines how many points to use for sampling plan
- Interpolation by covariance basis functions
- More statistical approach

anchored-ANOVA Collocation

- Dimension reduction inherent
- Sampling done on structured grid
- Sampling plan size dependent on number of design variables
- Polynomial interpolation
- More deterministic approach

Dimension Reduction for Kriging

- Kriging effective for $\mathcal{O}(10)$ design variables.
- For more design variables Kriging will defeat the purpose of having a surrogate in the first place.
- Fortunately, various engineering applications have shown that only a handful of design variables have non trivial impact on outputs of interest.
- How to identify the "important variables"?
- Morris' Algorithm.

Morris' Algorithm

- Premise: If the output parameter does not change with respect to a design variable then the variable can safely be ignored.
- Elementary effect $d_i(\mathbf{x})$ of design variable x_i:

$$d_i(\mathbf{x}) = \frac{f(x_1, x_2, ..., x_{i-1}, x_i + \Delta, x_{i+1}, ..., x_k) - f(\mathbf{x})}{\Delta}$$

- Choosing a set of $\mathbf{x}$ carefully, it is possible to calculate an elementary effect for each of k design variables using only $k+1$ function evaluations using the random orientation matrix $\mathbf{B}^*$:

$$\mathbf{B}^* = \left(\mathbf{1}_{k+1,1}\mathbf{x}^* + \frac{\Delta}{2}\left[\left(2\mathbf{B} - \mathbf{1}_{k+1,k}\right)\mathbf{D}^* + \mathbf{1}_{k+1,k}\right]\right)\mathbf{P}^*.$$

Morris' Algorithm

- r random orientation matrices are created to obtain r elementary effects for each design variable.
- Plot mean and standard deviation of each variable's effects.
- Variables with negligible effect on function will cluster around origin.
- Large fluctuations in standard deviation indicative of nonlinear and interactive effects.

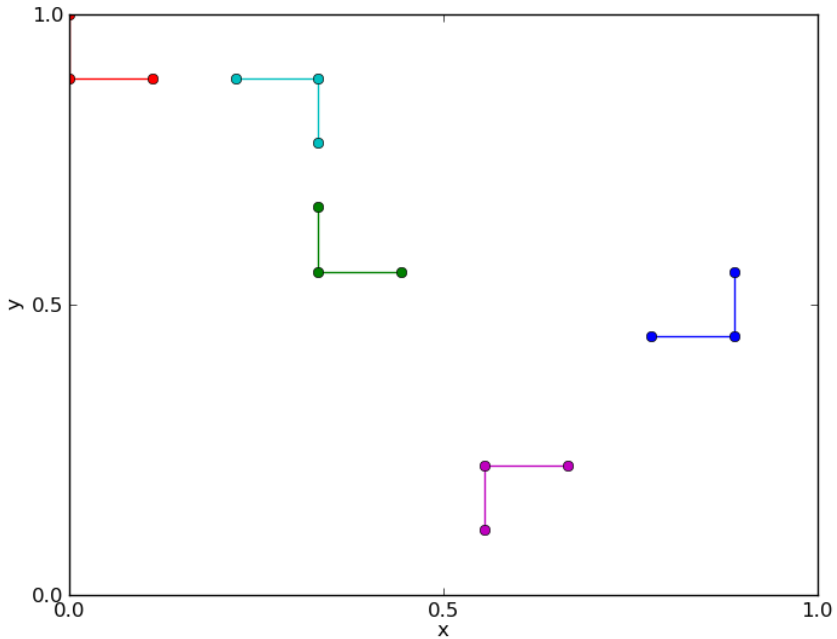

Designing a Kriging Sampling Plan

- All surrogate models are built around a set of points at which the objective computer code is actually evaluated.
- Intuitively, the surrogate accuracy is expected to decrease as one moves further away from such points.
- Important to spread N points as uniformly as possible across the design space.
- For Kriging, Latin Hypercube Sampling (LHS) is used to create a sampling plan.
- There is a notion of an optimized LHS sampling plan based on the maximin metric.

Latin Hypercube Sampling

- Basis of LHS rests upon dividing the normalized space of each design variable into n equally sized bins if n samples are required.
- As a result, when the n samples are taken it is guaranteed that the entire spectrum of each design variable's space has been visited.

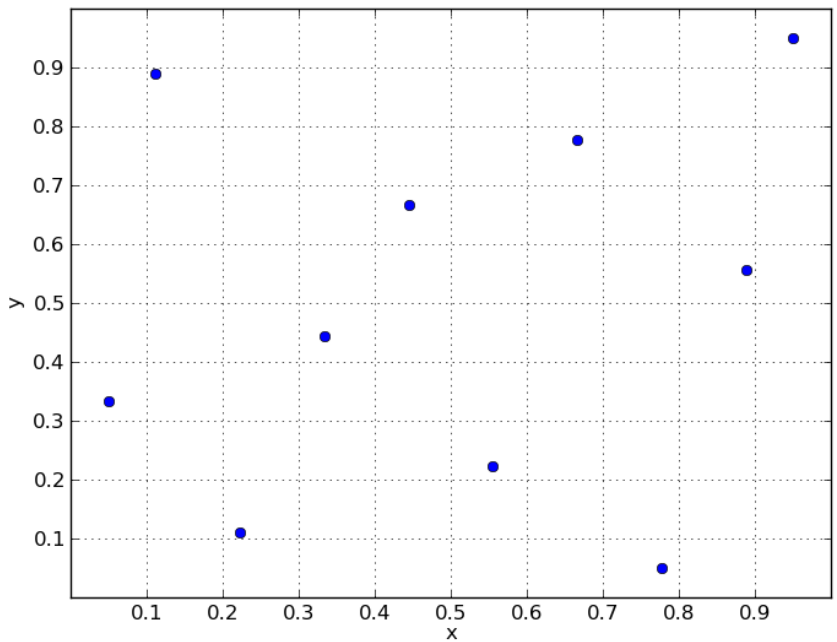

Optimizing a LHS Plan

- The maximin metric describe by Morris and Mitchell makes use of two notions in an attempt to quantify the 'space-fillingness' of a sampling plan.
- Unique distances between all points in the plan sorted in ascending order $\{d_1, d_2, ..., d_m\}$.
- Corresponding number of occurrences of each distance $\{J_1, J_2, ..., J_m\}$.
- In words, the Morris and Mitchell criteria states that an optimized sampling plan will minimize all J_i while maximizing the corresponding d_i.
- The maximin sampling plan maximizes d_1, and among plans for which this is true, minimizes J_1, among plans for which this is true, maximizes d_2,....

Optimizing a LHS Plan

- The previous definition can be restated into a pseudo equivalent minimization problem.

$$\Phi_q(\mathbf{X}) = \left(\sum_{j=1}^{m} J_j d_j^{-q} \right)^{1/q}$$

- The minimization of this equation and the Morris and Mitchell definition of the maximin sampling plan are used in unison to obtain a locally optimal sampling plan.
- Generate initial sampling plan, optimize for set of q values using simulated annealing.
- Resulting set of plans are contested directly against each other by explicit application of Morris and Mitchell's maximin definition.

Kriging on a Sampling Plan

- Optimized sampling plan $\mathbf{X} = \{\mathbf{x}^{(1)}, \mathbf{x}^{(2)}, ...\mathbf{x}^{(n)}\}$.
- At each datum $\mathbf{x}^{(k)}$ a random process $Y(\mathbf{x}^{(k)})$ induces an observation $y^{(k)}$.
- Resulting random field can be described with a mean value of $\mathbf{1}\mu$ and a correlation matrix,

$$\boldsymbol{\Psi} = \begin{pmatrix} cor[Y(\mathbf{x}^{(1)}), Y(\mathbf{x}^{(1)})] & \cdots & cor[Y(\mathbf{x}^{(1)}), Y(\mathbf{x}^{(n)})] \\ \vdots & \ddots & \vdots \\ cor[Y(\mathbf{x}^{(n)}), Y(\mathbf{x}^{(1)})] & \cdots & cor[Y(\mathbf{x}^{(n)}), Y(\mathbf{x}^{(n)})] \end{pmatrix}$$

$$cor[Y(\mathbf{x}^{(i)}), Y(\mathbf{x}^{(l)})] = \exp\left(-\sum_{j=1}^{k} \theta_j |x_j^{(i)} - x_j^{(l)}|^{p_j}\right)$$

Kriging on a Sampling Plan

- Given the formulation of the observations occurring at $\mathbf{x}^{(k)}$ as instances of a stochastic process, the likelihood of seeing the observed data is,

$$L\left(\mathbf{Y}^{(1)},...,\mathbf{Y}^{(n)}|\mu,\sigma,\{\theta_1,...,\theta_k\},\{p_1,...,p_k\}\right) =$$

$$\frac{1}{(2\pi\sigma^2)^{n/2}\left|\boldsymbol{\Psi}\right|^{1/2}} \times \exp\left[\frac{(\mathbf{y}-\mathbf{1}\mu)^T\boldsymbol{\Psi}^{-1}(\mathbf{y}-\mathbf{1}\mu)}{2\sigma^2}\right].$$

- Maximizing the log likelihood,

$$\hat{\mu} = \frac{\mathbf{1}^T\boldsymbol{\Psi}^{-1}\mathbf{y}}{\mathbf{1}^T\boldsymbol{\Psi}^{-1}\mathbf{1}}$$

$$\hat{\sigma}^2 = \frac{(\mathbf{y}-\mathbf{1}\mu)^T\boldsymbol{\Psi}^{-1}(\mathbf{y}-\mathbf{1}\mu)}{n}.$$

Kriging on a Sampling Plan

- Substitute $\hat{\sigma}$ and $\hat{\mu}$ into log likelihood to get, concentrated ln-likelihood function.

$$\log(L) \approx -\frac{n}{2}\log\left(\hat{\sigma}^2\right) - \frac{1}{2}\log|\mathbf{\Psi}|$$

- Optimize with respect to the θ and p parameters using global search algorithm.
- Once all optimizing parameters are available the goal is to utilize the parameters to build a model that makes function predictions on new points $\mathbf{x}$.

Making Predictions with Kriging Surrogate

- Construct a vector of correlations with existing points and $\mathbf{x}$,

$$\boldsymbol{\psi} = \begin{pmatrix} cor[Y(\mathbf{x}^{(1)}), Y(\mathbf{x})] \\ \vdots \\ cor[Y(\mathbf{x}^{(n)}), Y(\mathbf{x})] \end{pmatrix}.$$

- New predictions can be made at $\mathbf{x}$ using the maximum likelihood estimator,

$$\hat{y}(\mathbf{x}) = \hat{\mu} + \boldsymbol{\psi}^T \boldsymbol{\Psi}^{-1} (\mathbf{y} - \mathbf{1}\hat{\mu}).$$

- Prediction using kriging works to estimate a function value at a certain point by computing a weighted average of known function values in the vicinity of the objective points.

Collocation and anchored-ANOVA Algorithmic Overview

- anchored-ANOVA: Decompose objective function into functions of one variable $f(x_i)$, two variables $f(x_i, x_j)$, three variables $f(x_i, x_j, x_k)$ as needed.
- Collocation: For each component in the decomposition construct a polynomial interpolant by sampling objective function at pre-defined points.
- The pre-defined points are determined by Smolyak Sparse Grids, and a selection of quadrature abscissas (e.g. Newton-Cotes).
- Combine interpolants in decomposition to get an effective surrogate.

Numerical Interpolation in 1D

- First, pick a set of m_i collocation points.
- Evaluate objective function at all collocation points.
- Interpolated function is a linear expansion of some basis a_j^i (e.g. Lagrange polynomials) with weights $f\left(x_j^i\right)$.

$$U^i = \sum_{j=1}^{m_i} f\left(x_j^i\right) a_j^i$$

Clenshaw-Curtis Collocation Points

- Clenshaw-Curtis points consist of the extrema of Chebyshev polynomials.
- $n+1$ abscissas can exactly integrate polynomials of degree n.
- Points have the advantage of being nested.

$$x_j^i = \begin{cases} \cos\frac{\pi(j-1)}{m_i-1} & j = 1, \ldots, m_i \text{ if } i > 1 \\ 0 & j = 1 \text{ if } i = 1 \end{cases}$$

$$m_i = \begin{cases} 2^{i-1}+1 & i > 1 \\ 1 & i = 1 \end{cases}$$

Basis Functions

- Lagrange characteristic polynomials are plagued by the fact that each evaluation requires $\mathcal{O}(m_i^2)$ operations and often the computation is numerically unstable.
- Instead the barycentric form of Lagrange characteristic polynomials is used to form a basis.

$$a_j^i = \begin{cases} 1 & \text{if } i = 1 \\ \dfrac{\frac{w_j^i}{x - x_j^i}}{\sum_{j=0}^{m_i} \frac{w_j^i}{x - x_j^i}} & j = 1, ..., m_i \text{ for } i > 1 \end{cases}$$

- For Clenshaw-Curtis collocation points the barycentric weights are given by,

$$w_j^i = (-1)^{j+1} \delta_j^i \qquad \delta_j^i = \begin{cases} .5 & j = 1 \text{ or } j = m_i \\ 1 & \text{else} \end{cases}.$$

Expanding to Multivariate Interpolation

- Combine 1D interpolation formulas using tensor products
- Suffers from "Curse of Dimensionality".
- Mitigate the curse using Smolyak Sparse Grids.

$$\left(U^{i_1} \otimes \cdots \otimes U^{i_d}\right)(f) = \sum_{j_1=1}^{m_{i_1}} \cdots \sum_{j_d=1}^{m_{i_d}} f\left(x_{j_1}^{i_1}, \cdots, x_{j_d}^{i_d}\right)\left(a_{j_1}^{i_1} \otimes \cdots \otimes a_{j_d}^{i_d}\right)$$

Smolyak Sparse Grids

- Based on full tensor product formula the only difference being not all tensor products are used.
- In explicit form, the Smolyak formula is,

$$A_{q,d}(f) = \sum_{q-d+1 \leq |\mathbf{i}| \leq q} (-1)^{q-|\mathbf{i}|} \binom{d-1}{q-|\mathbf{i}|} \left(U^{i_1} \otimes \cdots \otimes U^{i_d}\right).$$

- i_k is the index corresponding to the level of interpolation in dimension k.
- The magnitude of $\mathbf{i}$ is $|\mathbf{i}| = |i_1 + \cdots + i_d|$.
- q keeps track of the level of interpolation of the Smolyak algorithm. More tensor product combinations are allowed as q increases.
- Smolyak algorithm reduces the total number of tensor product components by limiting the entries of $\mathbf{i}$.

Smolyak Sparse Grid Visualization

Level 4 Clenshaw-Curtis Full Tensor Product Grid

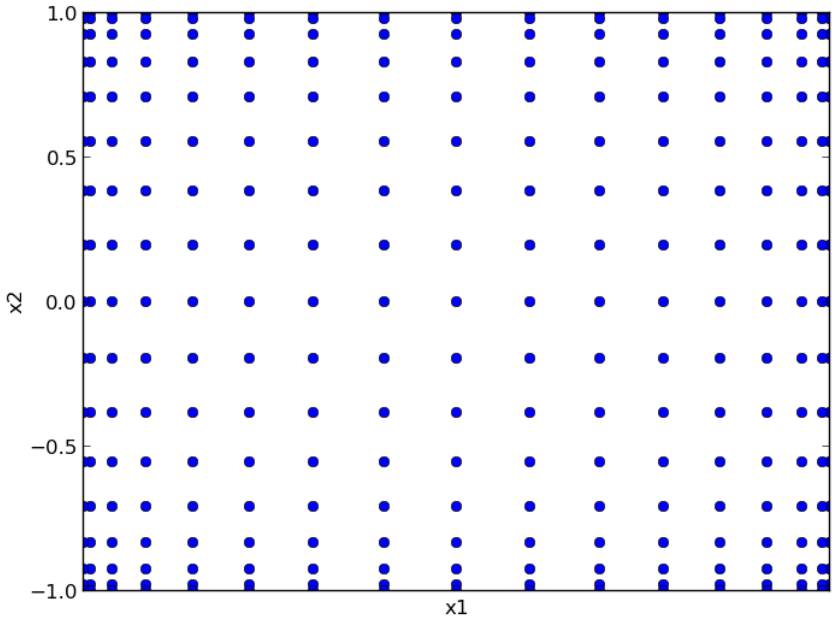

Level 4 Clenshaw-Curtis Smolyak Sparse Grid

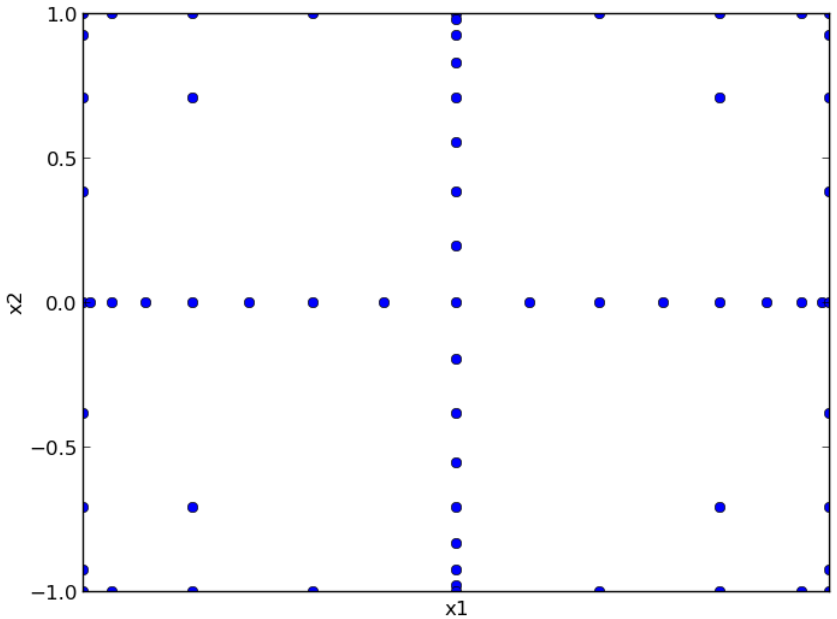

Smolyak Sparse Grid Visualization

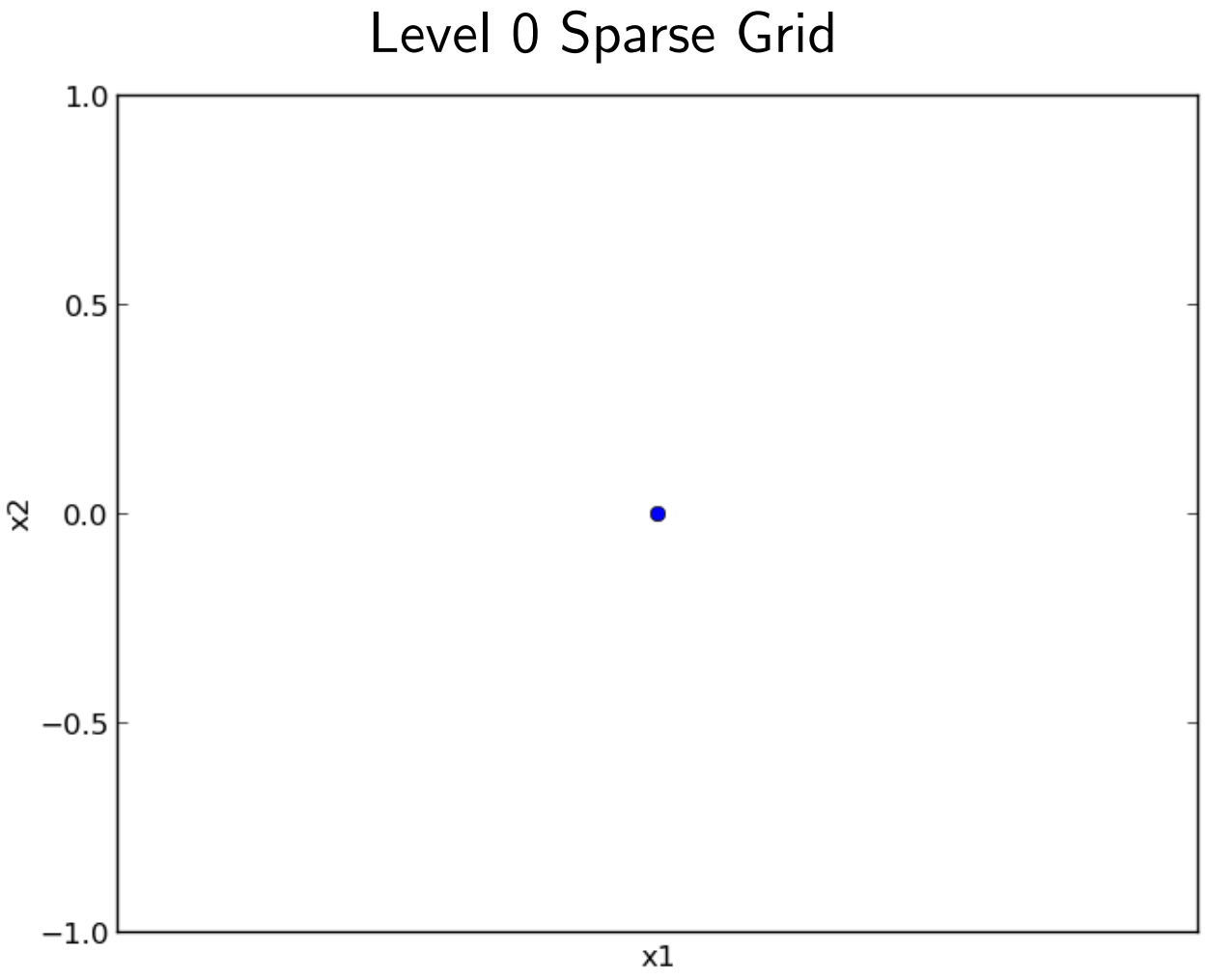

Smolyak Sparse Grid Visualization

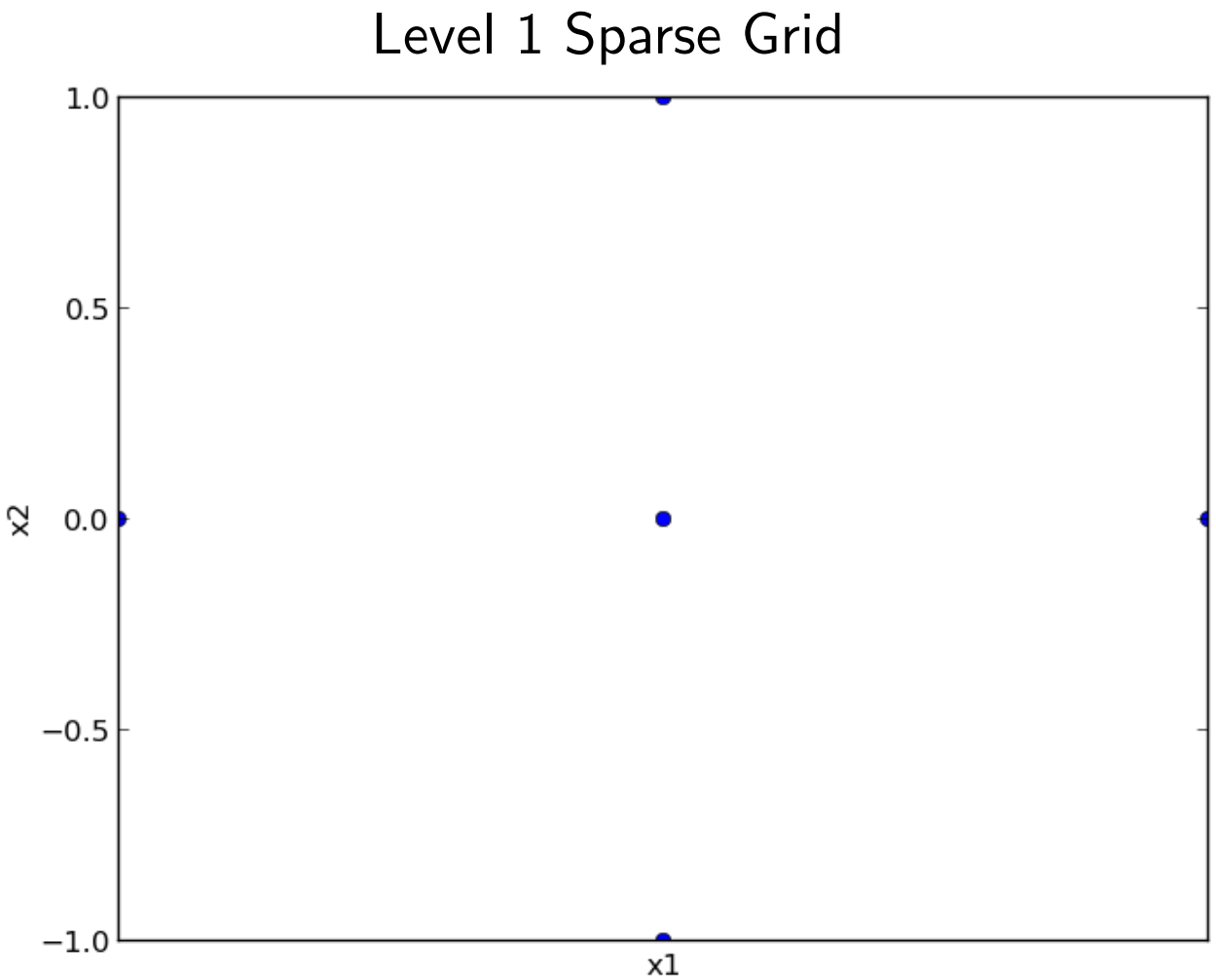

Smolyak Sparse Grid Visualization

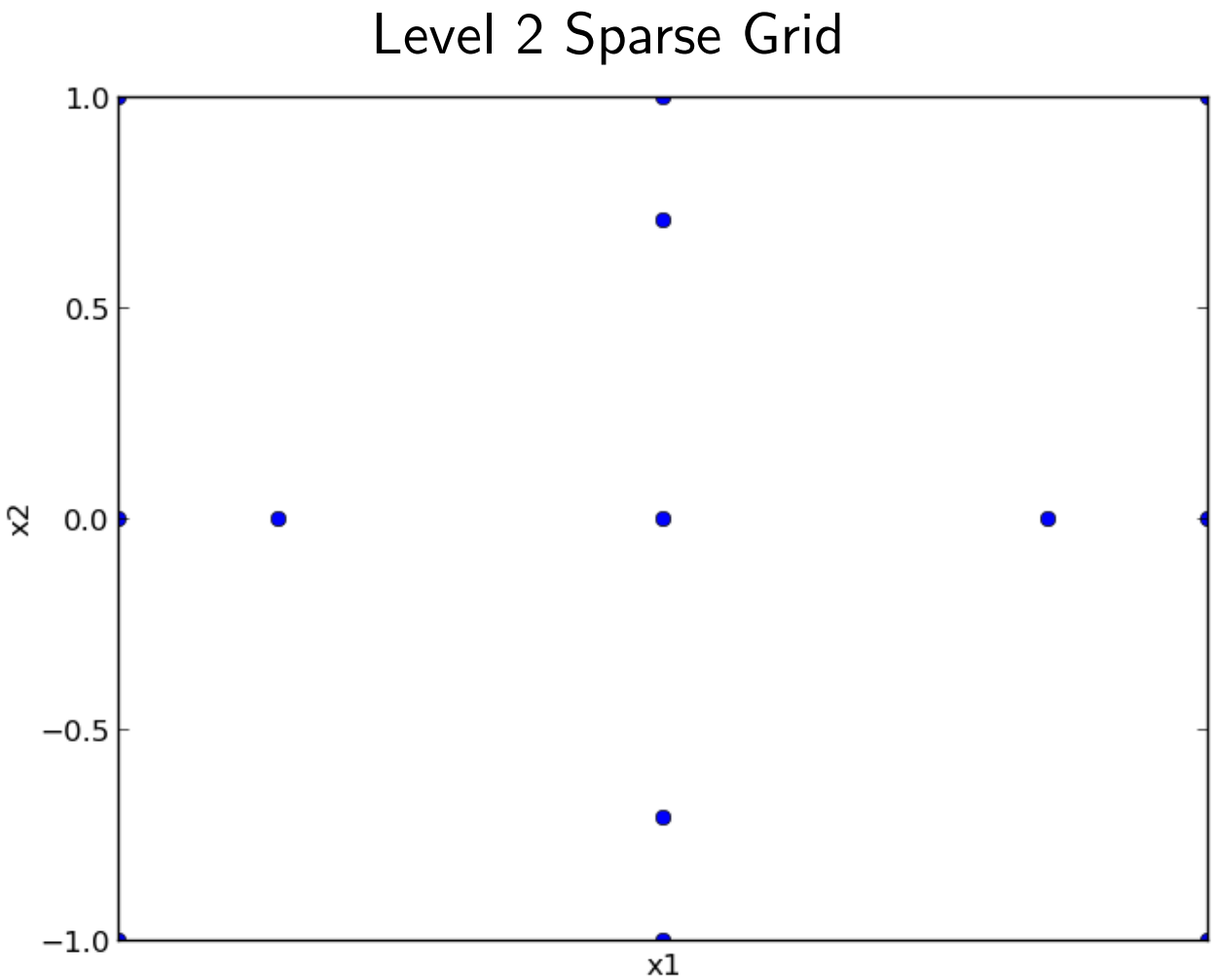

Smolyak Sparse Grid Visualization

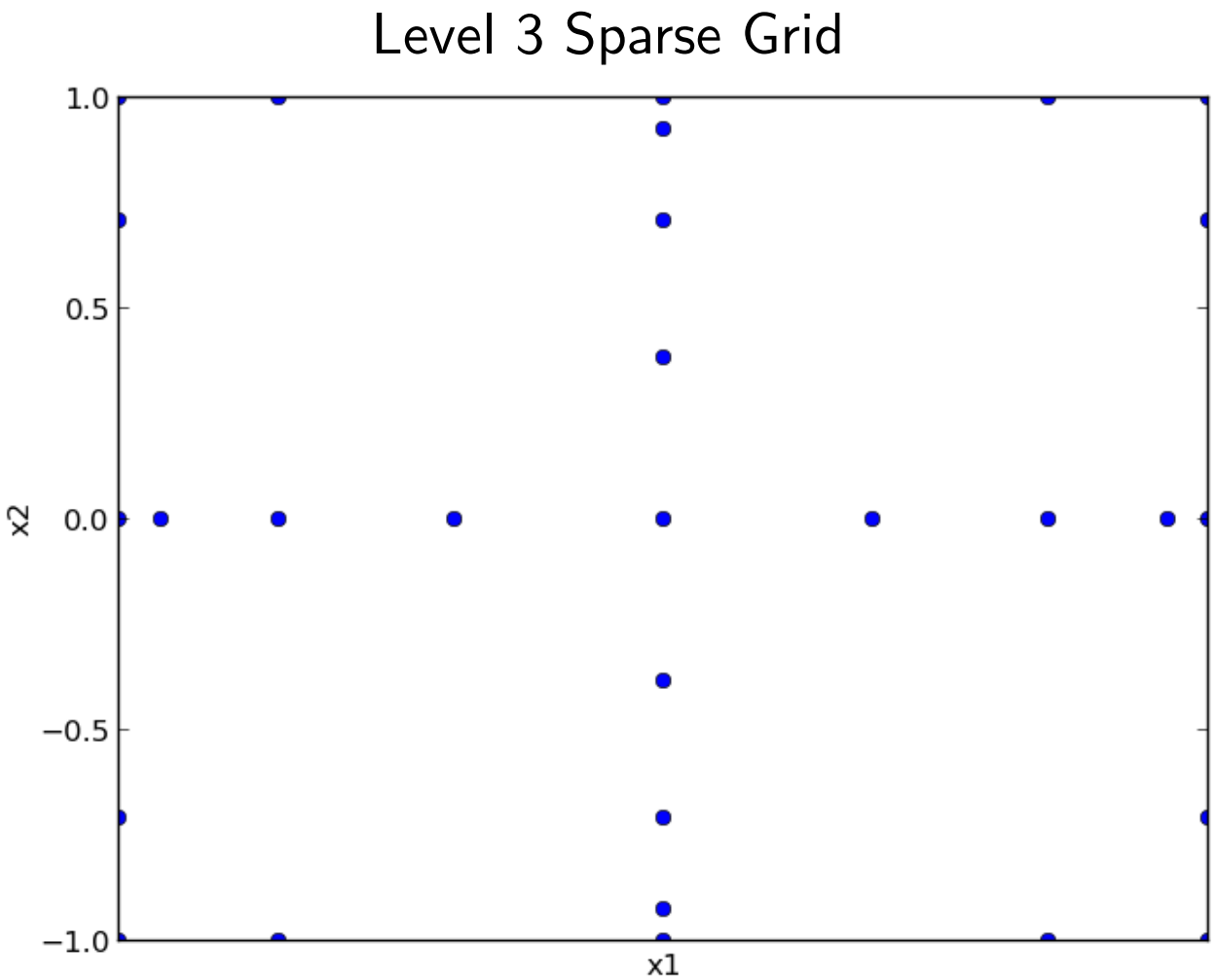

Smolyak Sparse Grid Visualization

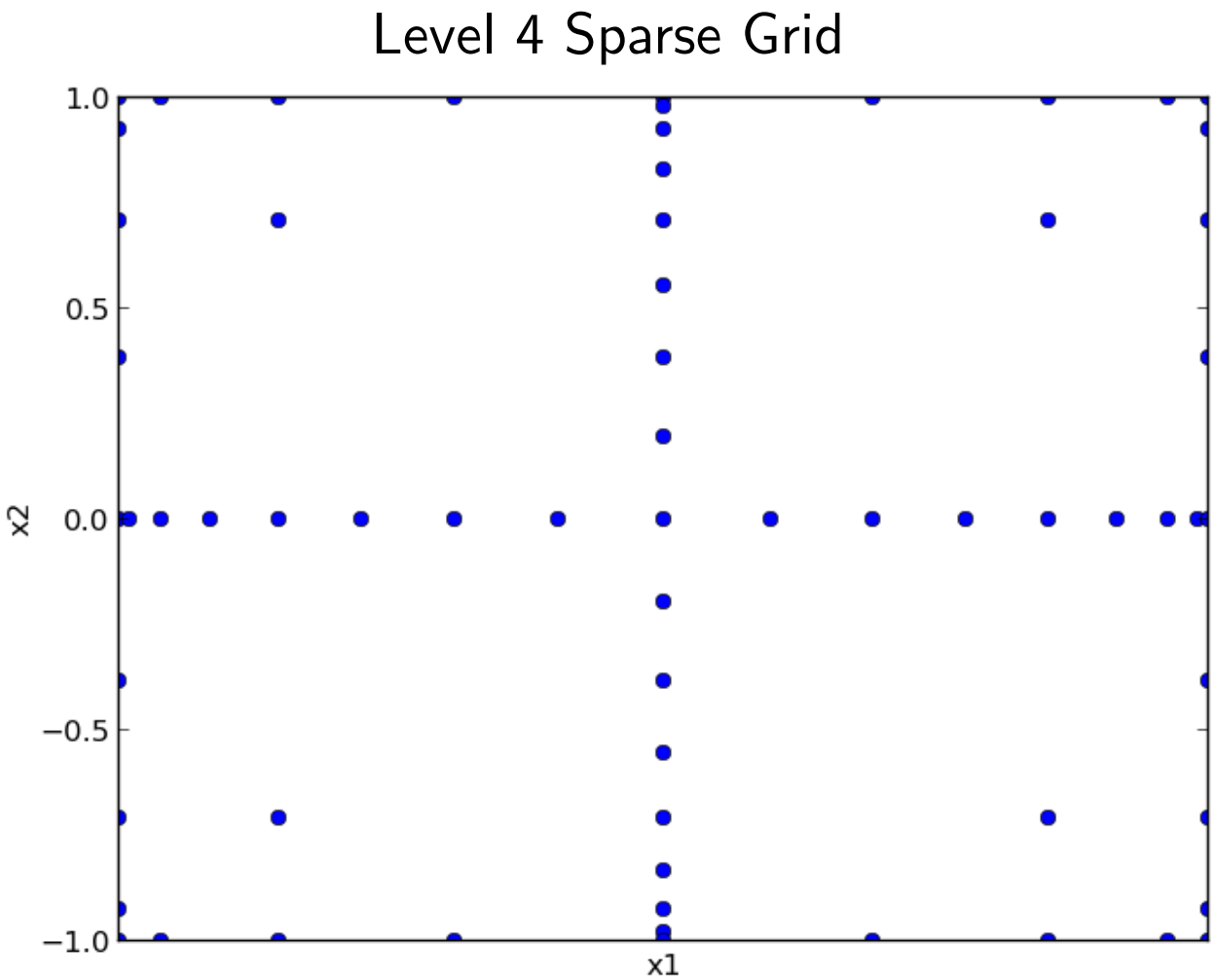

Smolyak Sparse Grid Visualization

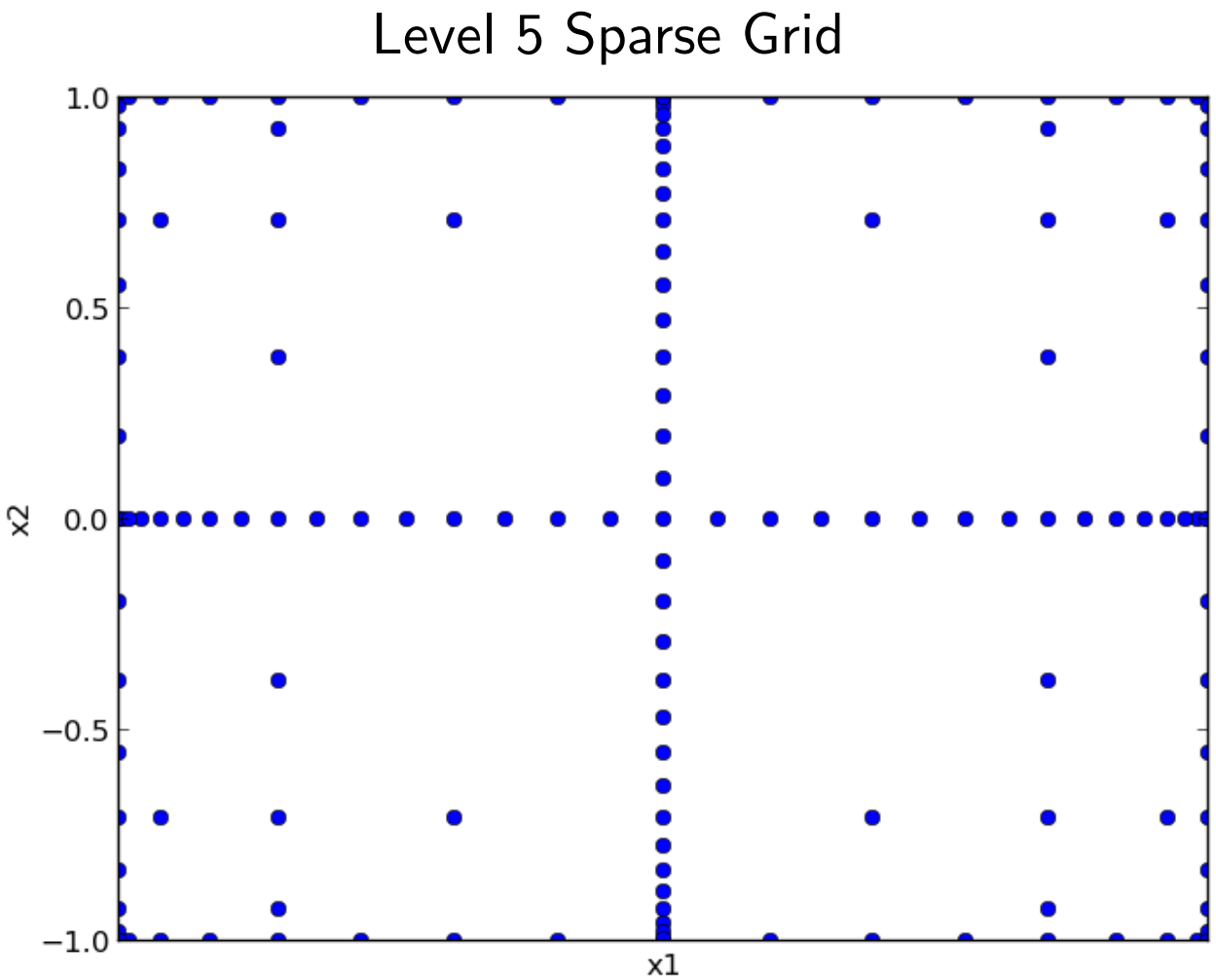

Smolyak Sparse Grid Visualization

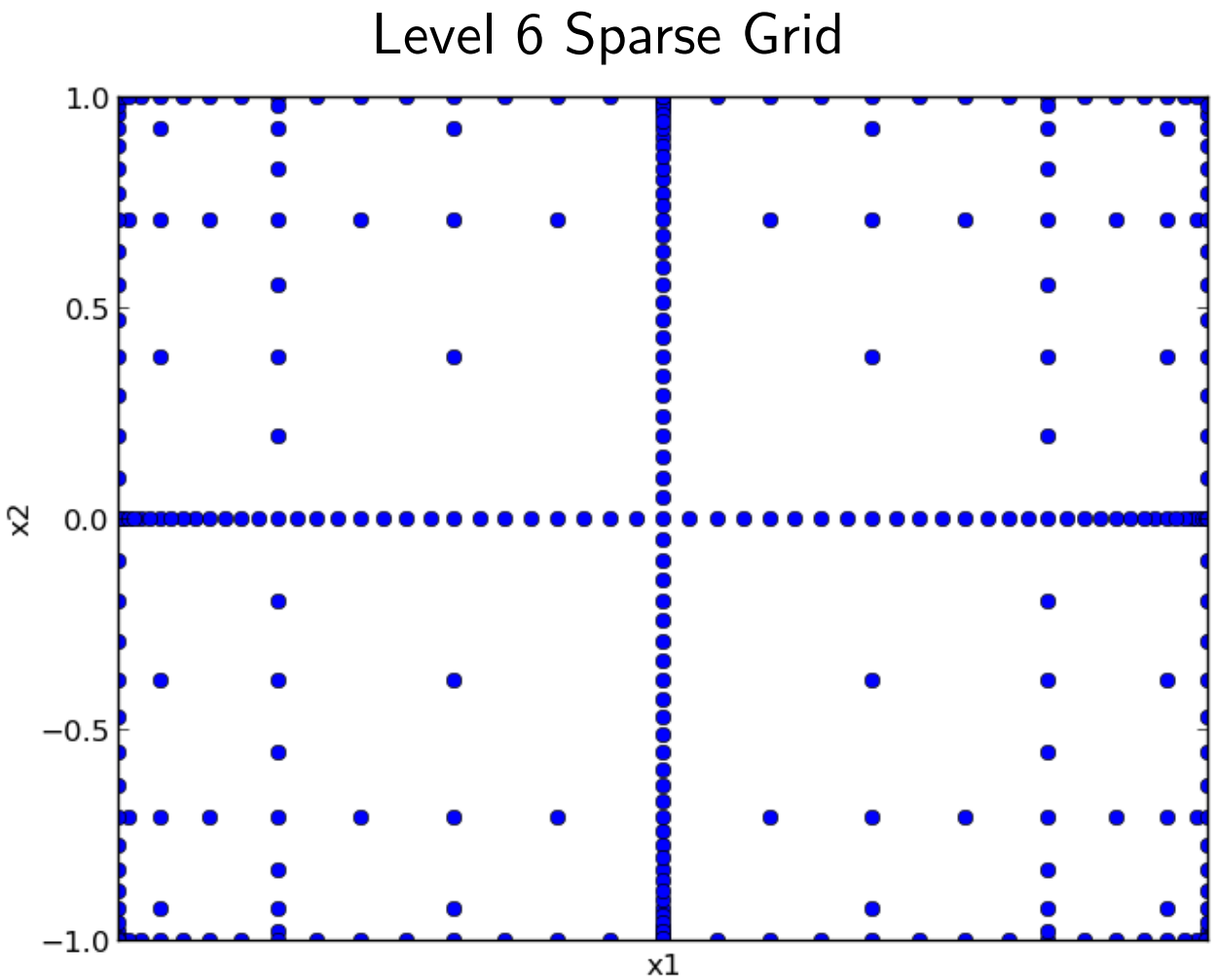

Smolyak Sparse Grid Visualization

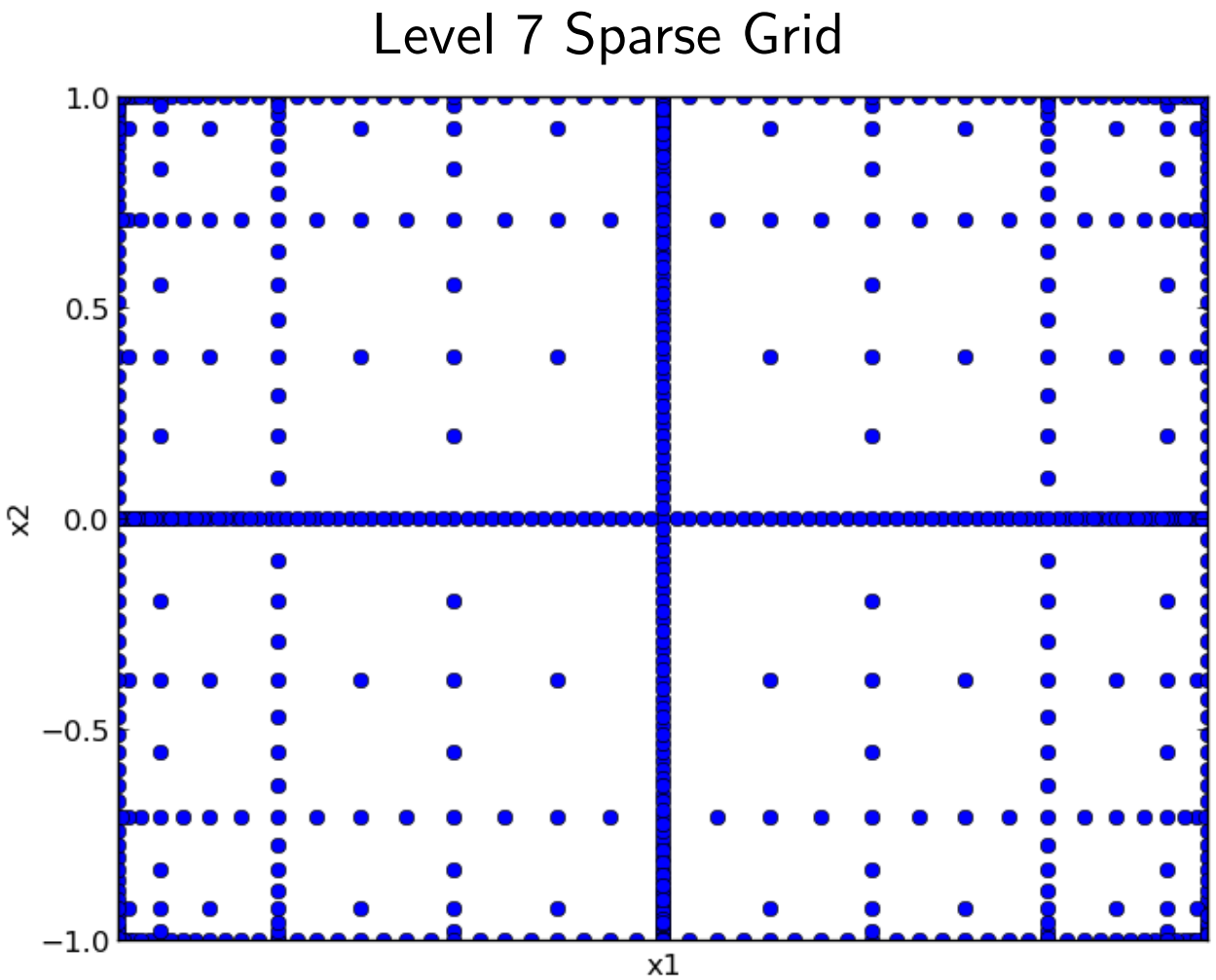

Recursive Definition of Smolyak's Algorithm

- The explicit definition of Smolyak's algorithm can be rewritten in a recursive fashion.
- Able to increase interpolation level without having to start over each time.
- Hierarchical surplus serves as an error indicator. Lets you know how well the interpolation is going as the grid is refined.
- Use hierarchical surplus to determine convergence.

$$A_{q,d}(f) = A_{q-1,d}(f) + \Delta A_{q,d}$$

$$\Delta A_{q,d} = \sum_{|\mathbf{i}|=q} \left(\underbrace{f(x_{j_1}^{i_1}, ..., x_{j_d}^{i_d}) - A_{q-1,d}(x_{j_1}^{i_1}, ..., x_{j_d}^{i_d})}_{\text{Hierarchical Surplus}} \right) \cdot \left(a_{j_1}^{i_1} \otimes \cdots \otimes a_{j_d}^{i_d} \right)$$

anchored-ANOVA Decomposition

- Consider a d-dimensional function $f(\mathbf{x}) = f(x_1, x_2, ..., x_d)$.
- The operator $P_{\mathbf{u}}$ projects from a d-dimensional space to a $|\mathbf{u}|$-dimensional space for some set $\mathbf{u} \subseteq \mathcal{D} = \{1, ..., d\}$.

$$f_{\mathbf{u}}(\mathbf{x}_{\mathbf{u}}) = P_{\mathbf{u}} f(\mathbf{x}) = \int_{\Omega^{d-|\mathbf{u}|}} f(\mathbf{x}) \, d\mu_{\mathcal{D}\setminus\mathbf{u}}(\mathbf{x})$$

- Use the Dirac measure $\delta(\mathbf{x} - \mathbf{a})d\mathbf{x}$ to evaluate the projection operator at an "anchor" point $\mathbf{a}$,

$$P_{\mathbf{u}} f(\mathbf{x}) = f(\mathbf{x})\,|_{\mathbf{x}=\mathbf{a}\setminus\mathbf{x}_{\mathbf{u}}}.$$

- For $\mathbf{u} \neq \mathbf{v}$ the following orthogonality relation holds:

$$(f_{\mathbf{u}}, f_{\mathbf{v}}) = 0$$

anchored-ANOVA Decomposition

- A function can be written in terms of its 2^d orthogonal components,

$$f(\mathbf{x}) = \sum_{\mathbf{u} \subseteq \mathcal{D}} f_{\mathbf{u}}(\mathbf{x}_{\mathbf{u}}).$$

- The component functions $f_{\mathbf{u}}$ are defined recursively,

$$f_{\mathbf{u}}(\mathbf{x}_{\mathbf{u}}) = P_{\mathbf{u}} f(\mathbf{x}) - \sum_{\mathbf{v} \subset \mathbf{u}} f_{\mathbf{v}}(\mathbf{x}_{\mathbf{v}}).$$

- Zeroth order component:

$$f_{\{\emptyset\}} = f(\overline{\mathbf{x}})$$

- First and second order components:

$$f_{\{x_i\}} = f(\mathbf{x})|_{\mathbf{x}=\mathbf{a}\setminus x_i} - f_{\{\emptyset\}}$$
$$f_{\{x_i,x_j\}} = f(\mathbf{x})|_{\mathbf{x}=\mathbf{a}\setminus\{x_i,x_j\}} - f_{\{\emptyset\}} - f_{\{x_i\}} - f_{\{x_j\}}$$

Note on anchored-ANOVA and Taylor Series

- The multivariate Taylor series of $f(\mathbf{x})$ about $\bar{\mathbf{x}}$,

$$f(\mathbf{x}) = f(\bar{\mathbf{x}}) + \sum_{i=1}^{d} \frac{\partial f(\mathbf{x})}{\partial x_i} (x_i - \bar{x}_i) + \frac{1}{2!} \sum_{i,j=1}^{d} \frac{\partial^2 f(\mathbf{x})}{\partial x_i \partial x_j} (x_i - \bar{x}_i)(x_j - \bar{x}_j) + \ldots$$

- Evaluate at $\mathbf{x} = \mathbf{a} \setminus x_i$,

$$f(\mathbf{x})|_{\mathbf{x}=\mathbf{a}\setminus x_i} = f(\bar{\mathbf{x}}) + \frac{\partial f(\mathbf{x})}{\partial x_i} (x_i - \bar{x}_i) + \frac{1}{2!} \frac{\partial^2 f(\mathbf{x})}{\partial x_i^2} (x_i - \bar{x}_i)^2 + \ldots$$

- Component functions are entire Taylor series expansions.
- Truncated anchored-ANOVA expansion will always be a better approximation than a truncated Taylor expansion.

Combining anchored-ANOVA and Smolyak Sparse Grids

- anchored-ANOVA decomposition forms foundation for surrogate model.
- Build each component function on a Smolyak sparse grid.
- Build all first-order components first.
- Compute sensitivity coefficient for each component.

$$\eta_i = \frac{\int_{\Omega_i} \left[f(\mathbf{x})|_{\mathbf{x}=\overline{\mathbf{x}}\setminus x_i} - f(\overline{\mathbf{x}}) \right] \rho(x_i) dx_i}{f_{\{\emptyset\}}}$$

- Build higher order components for only those variables whose sensitivity coefficients exceed a certain threshold.
- Continue to add higher order terms until convergence criteria met.

Outline

Infinite Lattice Problem Statement

- Reactor of infinite size is considered, effectively removing the effects of geometry in neutron transport
- System entirely characterized in terms of its material properties.
- Analytic solution available!

$$\begin{pmatrix} \Sigma_{a_1} + \Sigma_{1\to 2} & 0 \\ -\Sigma_{12} & \Sigma_{a_2} \end{pmatrix} \begin{pmatrix} \phi_1 \\ \phi_2 \end{pmatrix} = \frac{1}{k_\infty} \begin{pmatrix} \nu\Sigma_{f_1} & \nu\Sigma_{f_2} \\ 0 & 0 \end{pmatrix} \begin{pmatrix} \phi_1 \\ \phi_2 \end{pmatrix}$$

$$k_\infty = \frac{\Sigma_{a_2}\nu\Sigma_{f_1} + \Sigma_{1\to 2}\nu\Sigma_{f_2}}{\Sigma_{a_2}\left(\Sigma_{a_1} + \Sigma_{1\to 2}\right)}$$

Infinite Lattice Problem Statement

- Assume all variation in k_∞ can be attributed to its input cross sections, whose distributions follow a multivariate Gaussian.

			Correlation Coefficient Matrix				
	Mean	**Standard Dev.**	Σ_{a_1}	Σ_{a_2}	$\nu\Sigma_{f_1}$	$\nu\Sigma_{f_2}$	$\Sigma_{1\to2}$
Σ_{a_1}	1.04E-02	9.06E-05	1	0.07	-0.13	0.02	0.75
Σ_{a_2}	1.10E-01	2.31E-04	0.07	1	0.06	0.31	-0.07
$\nu\Sigma_{f_1}$	9.00E-03	4.85E-05	-0.13	0.06	1	0.33	-0.10
$\nu\Sigma_{f_2}$	1.91E-01	8.87E-04	0.02	0.31	0.33	1	0.01
$\Sigma_{1\to2}$	1.80E-02	2.18E-04	0.75	-0.07	-0.10	0.01	1

Infinite Lattice Problem Objective

- Propagate cross section uncertainties to find the mean and standard deviation of k_∞ using Monte Carlo sampling of true and surrogate functions, and the "Sandwich Equation".

$$\sigma^2(k_\infty) = S^T C S$$

$$S^T = \left(\begin{array}{ccccc} \frac{\partial k_\infty}{\partial \Sigma_{a_1}} & \frac{\partial k_\infty}{\partial \Sigma_{a_2}} & \frac{\partial k_\infty}{\partial \nu\Sigma_{f_1}} & \frac{\partial k_\infty}{\partial \nu\Sigma_{f_2}} & \frac{\partial k_\infty}{\partial \Sigma_{1\to 2}} \end{array} \right)$$

- Also, find sensitivity coefficients analytically and numerically.

$$\left.\frac{\partial k_\infty}{\partial \Sigma_i}\right|_{\Sigma_{j\neq i}=\bar{\Sigma}_j} \approx \frac{k_\infty(\Sigma_i + \Delta\Sigma_i) - k_\infty(\Sigma_i - \Delta\Sigma_i)}{2\Delta\Sigma_i}$$

Convergence of 5-D Sparse Grid Interpolant

Hierarchical Surplus

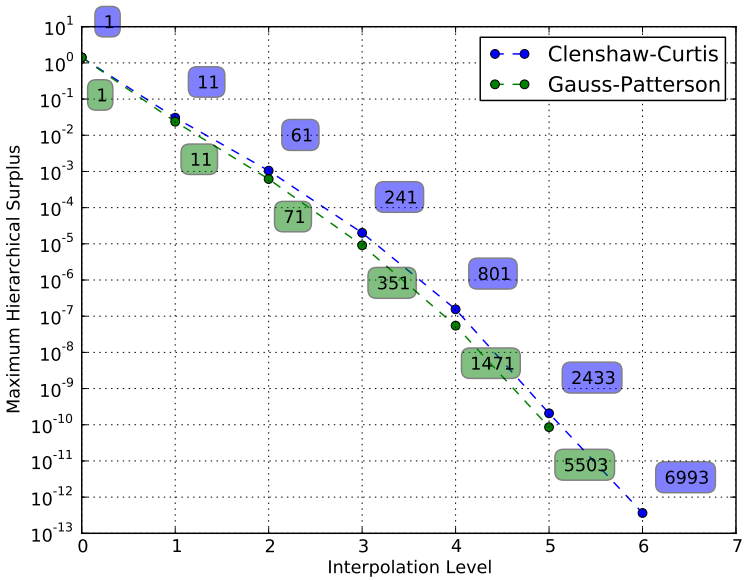

Number of Abscissas

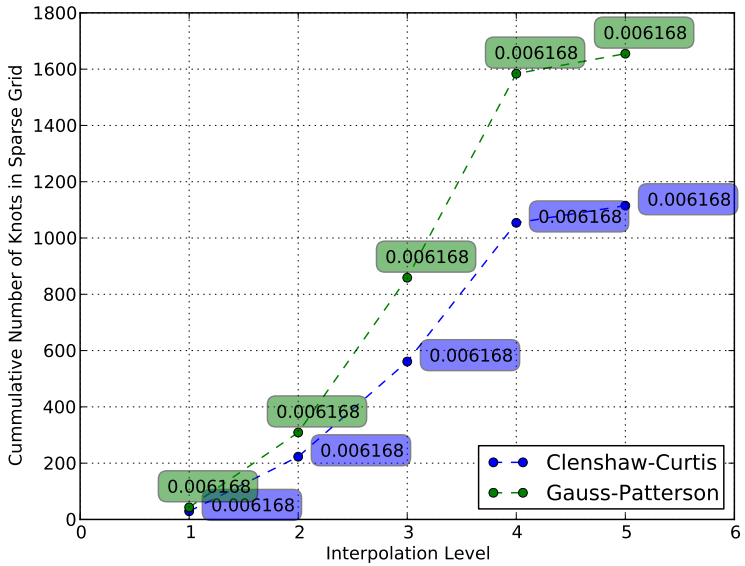

Mean and Variance of k_∞

- 1000 Monte Carlo samples, using the same random numbers, were gathered for each method.
- In "1D ANOVA" only the 5 first-order components are used.
- In "All ANOVA" all 32 components are used.
- Clenshaw-Curtis collocation points represented by "CC" while "GP" is Gauss-Patterson.

Method	**Mean**	**99% CI**	**Standard Dev.**	**99% CI**
5D Sparse Grid CC	1.41562	(1.41512, 1.41612)	0.006168	(0.005909, 0.006544)
5D Sparse Grid GP	1.41562	(1.41512, 1.41612)	0.006168	(0.005831, 0.006544)
1D ANOVA CC	1.41560	(1.41510, 1.41610)	0.006168	(0.005831, 0.006544)
All ANOVA CC	1.41562	(1.41512, 1.41612)	0.006168	(0.005831, 0.006544)
1D ANOVA GP	1.41560	(1.41510, 1.41610)	0.006168	(0.005831, 0.006544)
All ANOVA GP	1.41562	(1.41512, 1.41612)	0.006168	(0.005831, 0.006544)
True Function	1.41562	(1.41512, 1.41612)	0.006168	(0.005831, 0.006544)
Sandwich			0.006540	

Sensitivity Coefficients for k_∞

- Central differencing... perturbations (1%) made to each cross section while holding the others at mean value.
- Models differ from analytic coefficients in fourth decimal place
- Expected due to $\mathcal{O}(\Delta\Sigma^2)$ convergence of central differencing.

	Normalized Sensitivity Coefficient of k_∞				
Method	Σ_{a_1}	Σ_{a_2}	$\nu\Sigma_{f_1}$	$\nu\Sigma_{f_2}$	$\Sigma_{1\to 2}$
5D Sparse Grid CC	-.367551	-.776087	.224060	.776010	.143491
5D Sparse Grid GP	-.367551	-.776087	.224060	.776010	.143491
1D ANOVA CC	-.367556	-.776098	.224063	.776020	.143493
All ANOVA CC	-.367551	-.776087	.224060	.776010	.143491
1D ANOVA GP	-.367556	-.776098	.224063	.776020	.143493
All ANOVA GP	-.367551	-.776087	.224060	.776010	.143491
Analytic	-.367520	-.775956	.224044	.775956	.143476
Central Difference	-.367551	-.776089	.224060	.776011	.143492

Kriging Surrogate for k_∞

- Observe that for ten evaluation points, twice the number of design variables in the objective function, error goes to zero.

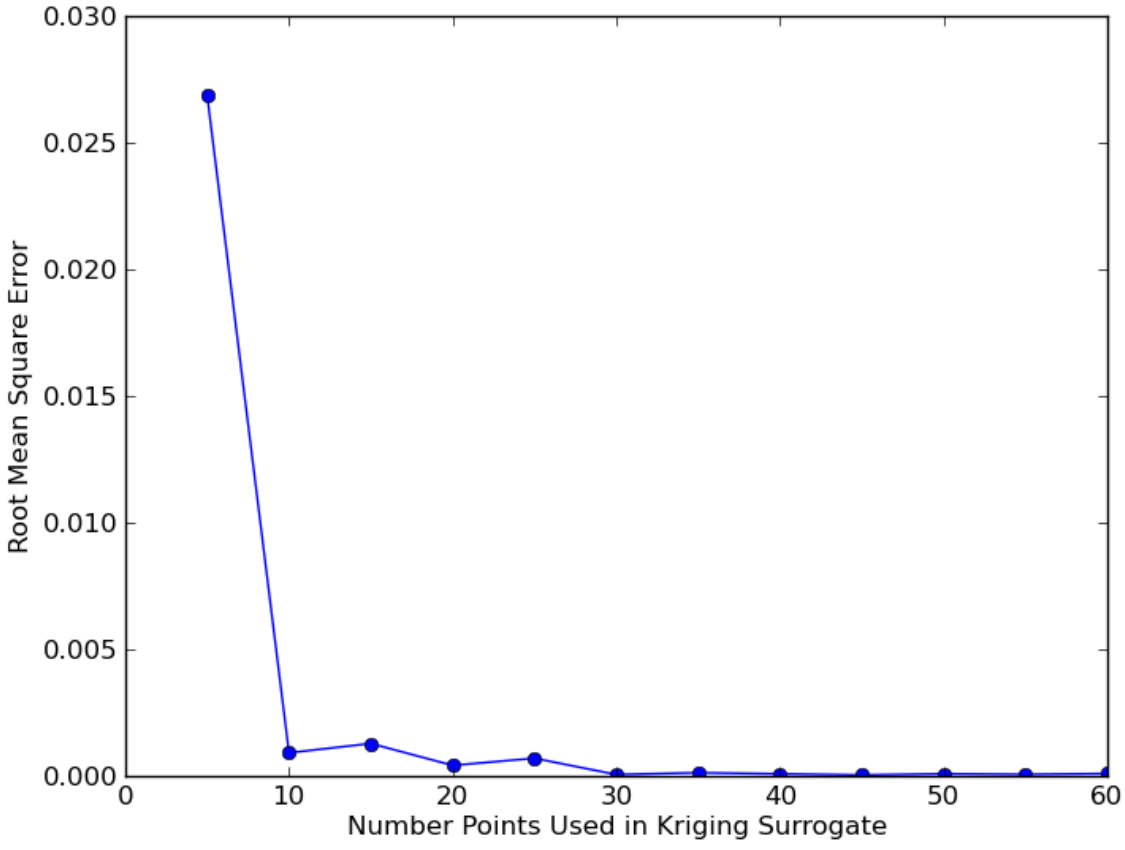

Point Kinetics/Lumped Thermal Hydraulics Problem Statement

- Modeling a transient resulting from a half sawtooth external reactivity insertion in a BN800 sodium fast cooled reactor.

$$\rho_{ex}(t) = \begin{cases} t\rho_{max}/20 & t \leq 20 \\ 0 & t > 20 \end{cases}$$

- The physical model of the reactor consists of point kinetics to model the neutronics and lumped thermal hydraulics equations to describe temperature feedback.
- The coupled system is nonlinear and only has a time dependence.
- Kinetics coupled to thermal hydraulics through reactivity.

$$\rho(T_f, T_c, t) = \rho_{ex} + \alpha_d(T_f - T_f(0)) + \alpha_c(T_c - T_c(0))$$

Point Kinetics/Lumped Thermal Hydraulics Problem Statement

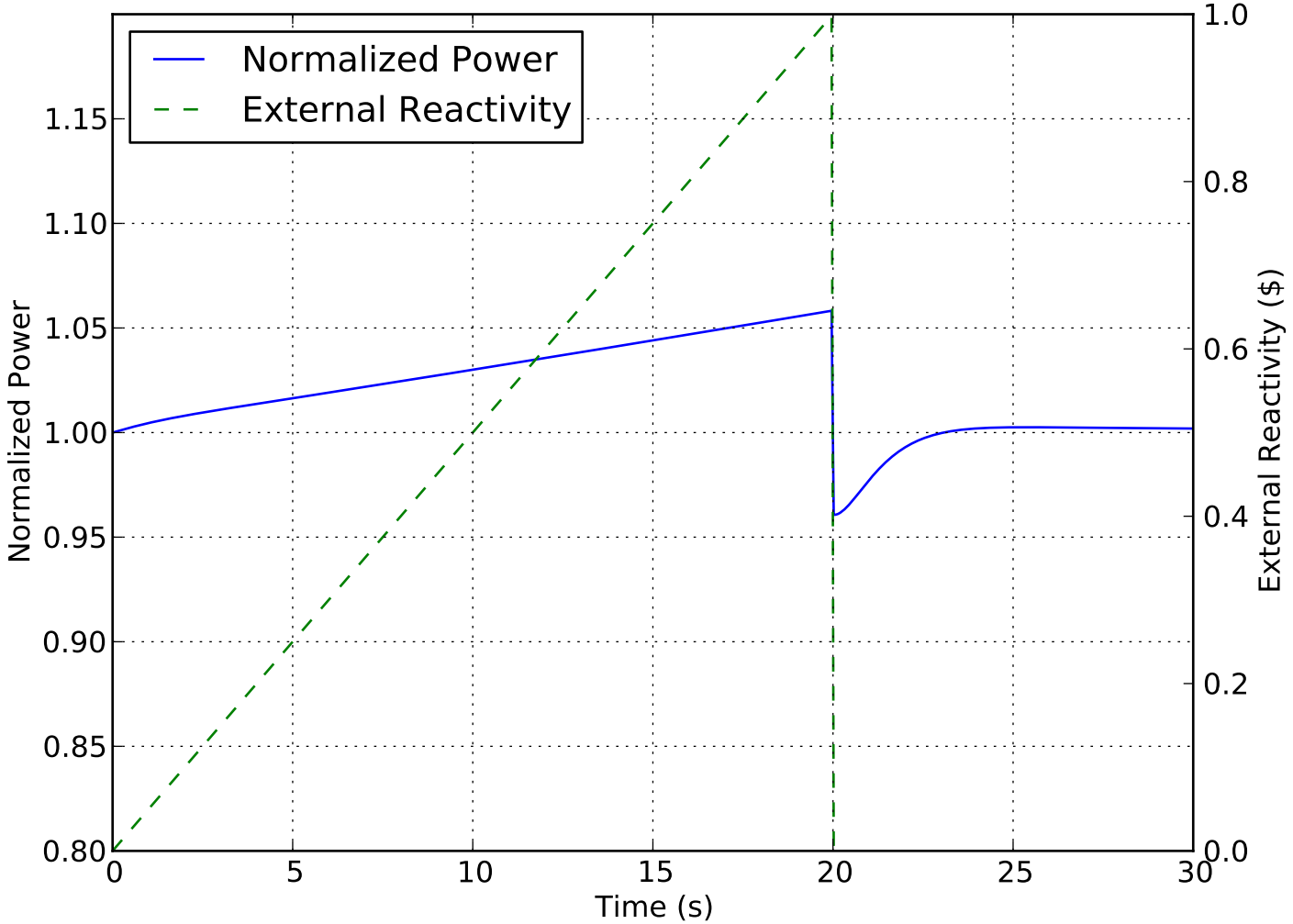

Point Kinetics/Lumped Thermal Hydraulics Problem Statement

- Reactor Power

$$\frac{dP}{dt} = \frac{\rho(T_f, T_c, t) - \beta}{\Lambda} P + \sum_{k=1}^{6} \lambda_k C_k$$

- Precursor Concentration

$$\frac{dC_k}{dt} = -\lambda_k C_k + \frac{\beta_k}{\Lambda} P$$

- Fuel Temperature

$$M_f c_{pf} \frac{dT_f}{dt} = P + Ah(T_c - T_f)$$

- Coolant Temperature

$$M_c c_{pc} \left(\frac{dT_c}{dt} + v \frac{T_c - T_{in}}{L} \right) = Ah(T_f - T_c)$$

Point Kinetics/Lumped Thermal Hydraulics Objective

- A total of twenty two random variables will be investigated for their affect on the maximum fuel temperature attained during transient.

$$\lambda_1, \lambda_2, \lambda_3, \lambda_4, \lambda_5, \lambda_6, \beta_1, \beta_2, \beta_3, \beta_4, \beta_5, \beta_6$$
$$\Lambda, Ah, M_c, M_f, c_{pc}, c_{pf}, v, \alpha_d, \alpha_c, \rho_{max}$$

- All random variables are assumed to be independent of one another.
- Objective is to identify "important variables", perform sensitivity analysis, and calculate basic statistics using anchored-ANOVA collocation and Kriging.

anchored-ANOVA Sensitivity Analysis

- For each first-order component in anchored-ANOVA decomposition, calculate a sensitivity coefficient.
- Variables Ah, α_d, and ρ_{max} comprise 82% of the total sensitivity.

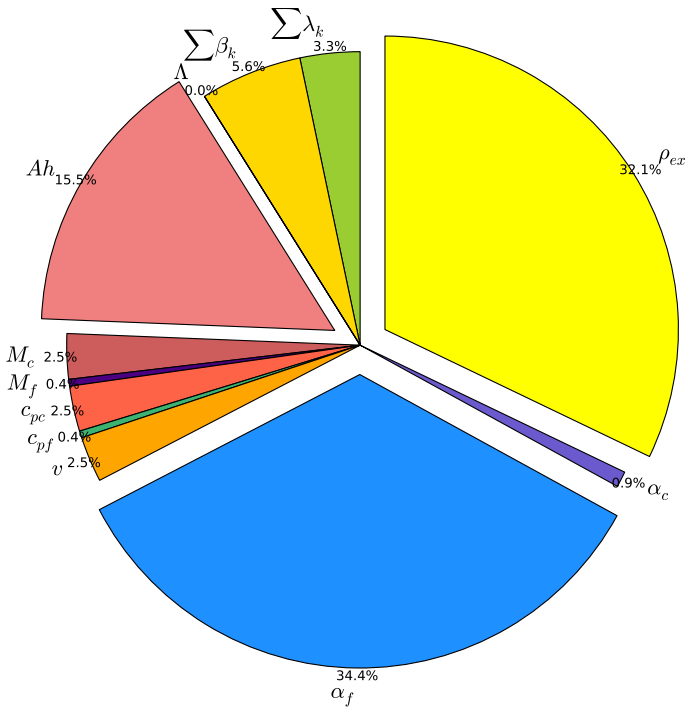

Morris' Algorithm Sensitivity Analysis

- Algorithm visually identifies Ah, α_d, and ρ_{max} to be "important variables".

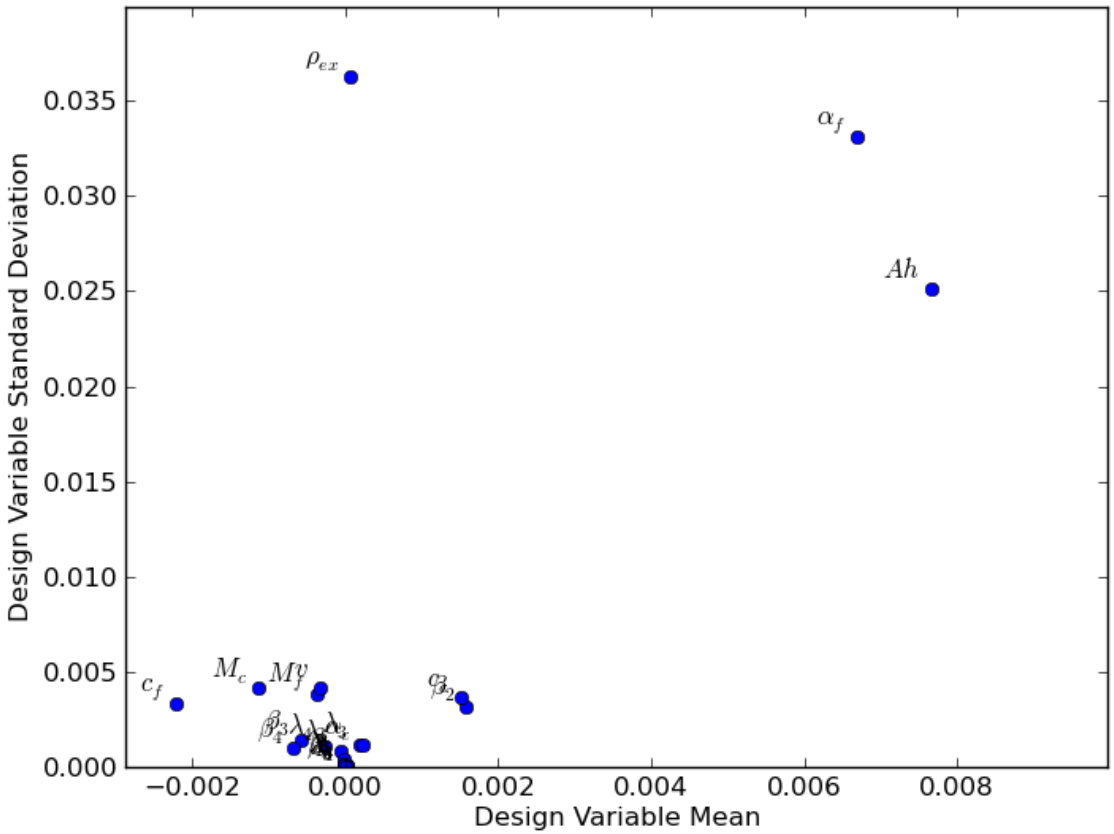

Statistics from anchored-ANOVA Collocation Surrogate

- Basic statistics for the maximum fuel temperature attained during transient.
- A total of 1000 Monte Carlo samples were used to get the statistics for each method (using the same random numbers).
- A Kriging surrogate based on 3 "important variables" was constructed and also sampled 1000 times for a mean normalized temperature of 1.03198 ± 0.002299.

Method	**Mean**	**99% CI**	**Standard Dev.**	**99% CI**
1D ANOVA CC	1.03193	(1.03175, 1.03211)	0.002187	(0.002068, 0.002320)
All ANOVA CC	1.03193	(1.03175, 1.03211)	0.002196	(0.002076, 0.002330)
1D ANOVA GP	1.03193	(1.03175, 1.03211)	0.002187	(0.002068, 0.002320)
All ANOVA GP	1.03193	(1.03175, 1.03211)	0.002196	(0.002076, 0.002330)
True Function	1.03193	(1.03175, 1.03211)	0.002196	(0.002076, 0.002330)

Statistics from anchored-ANOVA Collocation Surrogate

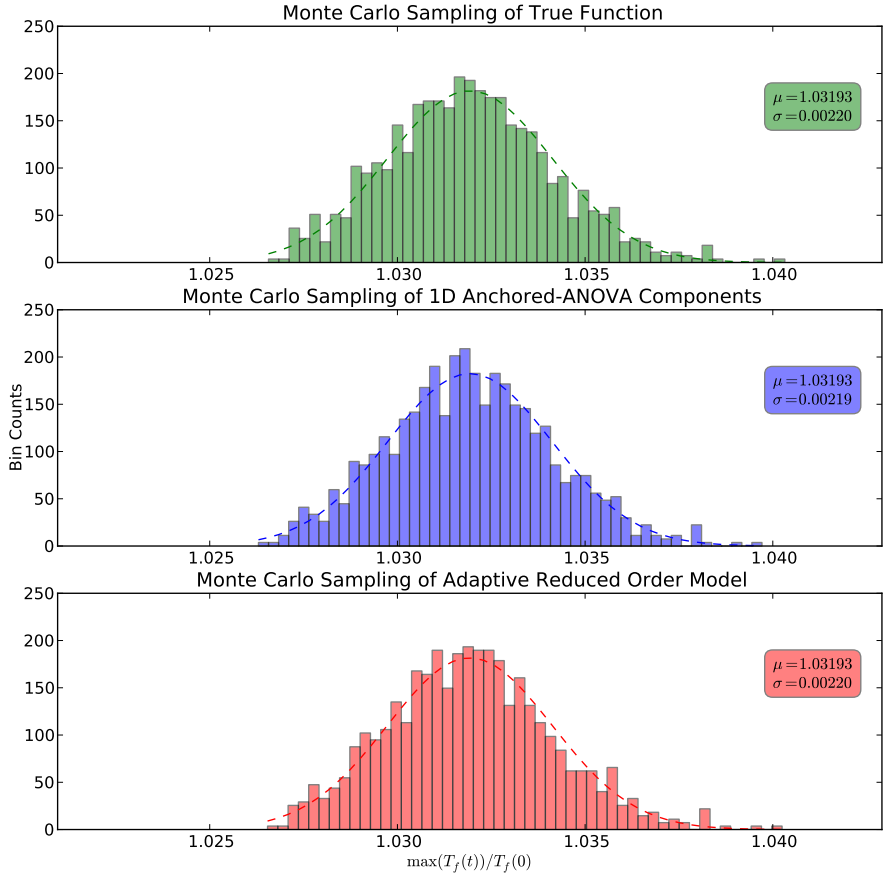

Statistics from anchored-ANOVA Collocation Surrogate

- Higher-order ANOVA components built only to model interaction effects between Ah, α_d, and ρ_{max}.
- Surrogate consisting entirely of first-order components required 126 function evaluations.

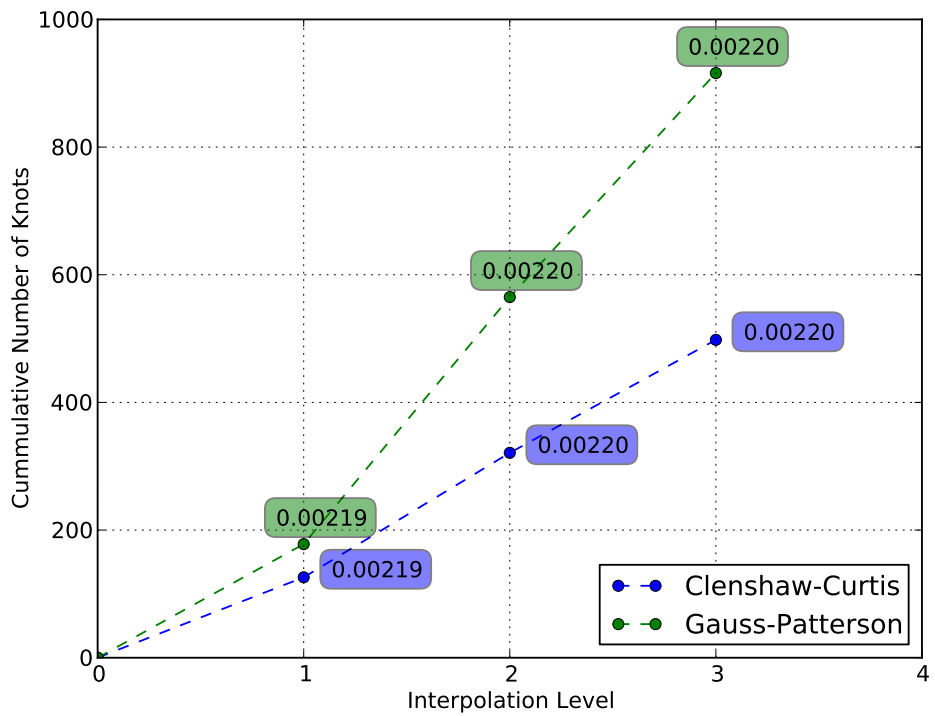

Calculating Sensitivity Coefficients on anchored-ANOVA Collocation Surrogates

Random Variable	1D ANOVA CC	All ANOVA CC	Central Diff.
λ_4	9.7308E-04	9.7309E-04	9.7379E-04
β_2	-2.6582E-03	-2.6582E-03	-2.6616E-03
Λ	-8.9294E-08	-8.9295E-08	-8.9364E-08
Ah	1.2553E-02	1.2553E-02	1.2584E-02
M_c	1.8753E-03	1.8753E-03	1.8716E-03
M_f	-3.6695E-04	-3.6695E-04	-3.6360E-04
c_{pc}	1.8753E-03	1.8753E-03	1.8903E-03
c_{pf}	-3.6695E-04	-3.6695E-04	-3.5976E-04
v	1.8838E-03	1.8839E-03	1.9177E-03
α_d	-2.6655E-02	-2.6656E-02	-2.6625E-02
α_c	8.4387E-04	8.4387E-04	8.7194E-04
ρ_{max}	3.1164E-02	3.1164E-02	3.1272E-02

Three Mile Island (TMI) Minicore Problem Statement

- Build surrogate for TMI Minicore power distribution using core simulator code PARCS.
- Total of 25 homogenized, two-group cross sections are used as design variables.

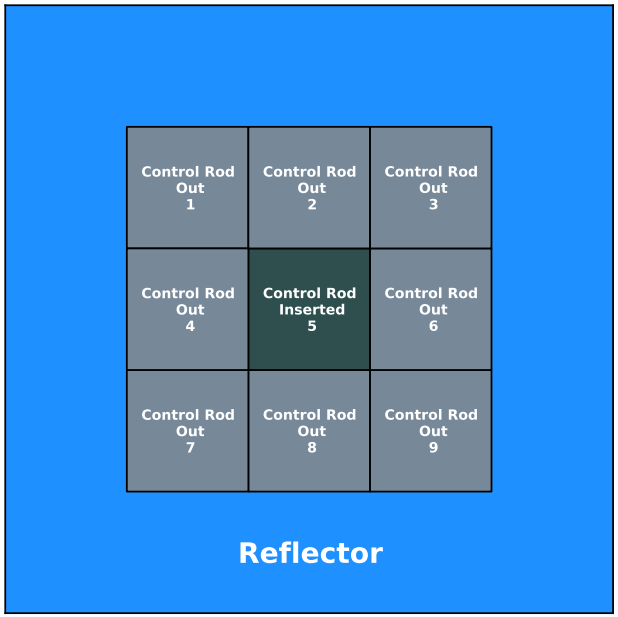

TMI Minicore Problem Data

- The few group, homogenized cross section description for each fuel assembly consists of transport, absorption, nu-fission, and scatter cross sections along with values for ADFs.
- For a two-group problem the total number of cross sections to describe an assembly is nine.
- Since the homogenized reflector region does not support fission only seven homogenized cross sections are required to describe it.
- Few-group covariance matrix is obtained using the 'Two-Step' method based on a total of 300 transport calculations with perturbed multigroup cross sections.

Morris' Algorithm Sensitivity Study

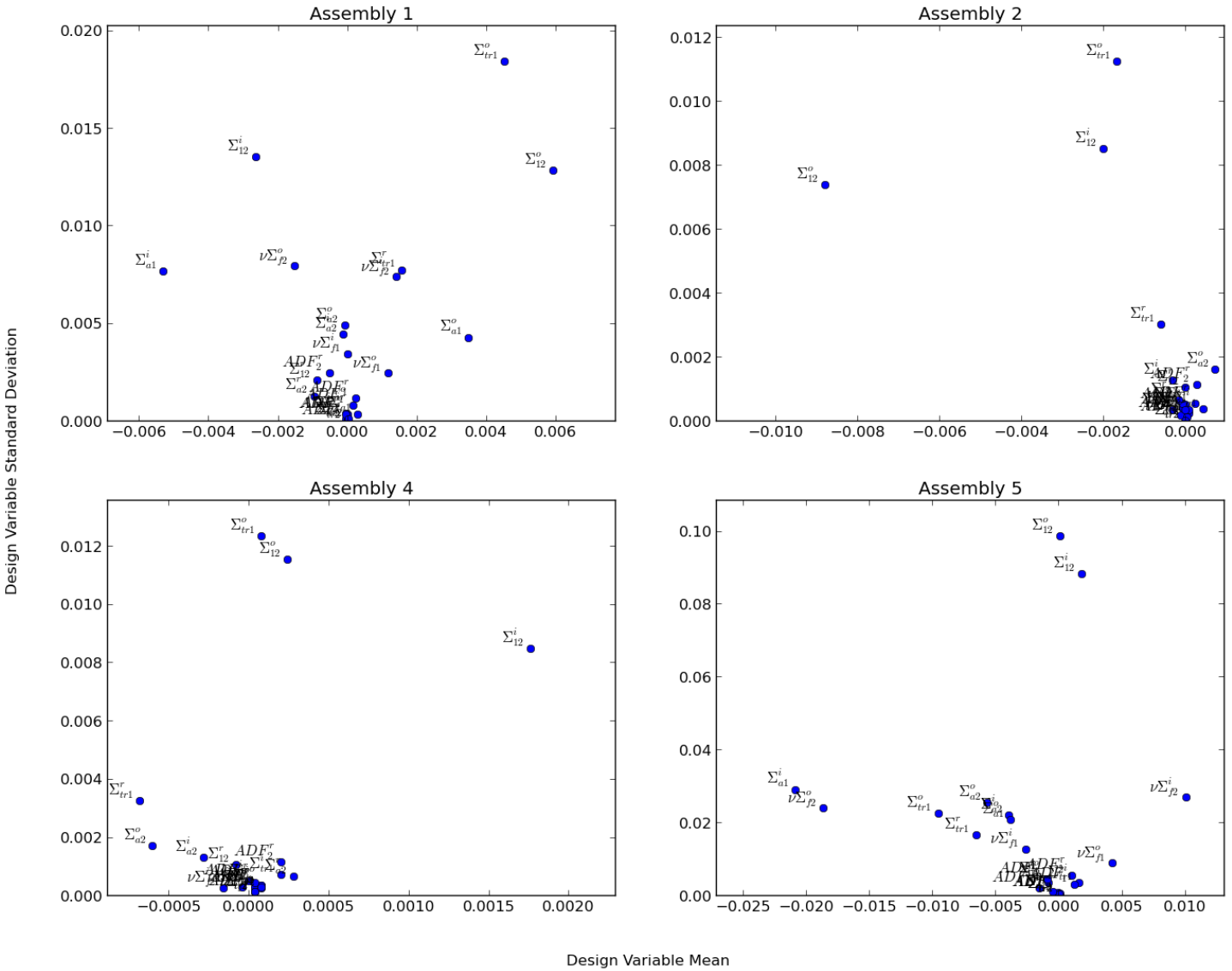

Kriging Surrogate

- Kriging surrogate is constructed for the core power as a function of Σ^i_{a1}, $\nu\Sigma^i_{f2}$, Σ^i_{12}, Σ^o_{tr1}, $\nu\Sigma^o_{f2}$ and Σ^o_{12}.
- Using these variables a sampling plan consisting of 20 true PARCS evaluations was designed.
- Based on the optimized sampling plan a Kriging surrogate was constructed and sampled 500 times in accordance with the six design variables' covariance matrix.

Sampling the Kriging Surrogate

Kriging Surrogate Statistics

Assembly	Mean	99% CI	Standard Dev.
1	0.8385	(0.8384, 0.8386)	0.0010
2	1.1499	(1.1497, 1.1500)	0.0013
3	0.8384	(0.8383, 0.8386)	0.0010
4	1.1499	(1.1497, 1.1500)	0.0013
5	1.0465	(1.0462, 1.0467)	0.0022
6	1.1499	(1.1497, 1.1500)	0.0013
7	0.8384	(0.8383, 0.8386)	0.0010
8	1.1499	(1.1497, 1.1500)	0.0013
9	0.8384	(0.8383, 0.8386)	0.0010

PARCS Two-Step Statistics

Assembly	Mean	99% CI	Standard Dev.
1	0.8387	(0.8386, 0.8388)	0.0007
2	1.1499	(1.1498, 1.1500)	0.0011
3	0.8387	(0.8386, 0.8388)	0.0007
4	1.1499	(1.1498, 1.1500)	0.0011
5	1.0453	(1.0450, 1.0456)	0.0027
6	1.1499	(1.1498, 1.1500)	0.0011
7	0.8387	(0.8386, 0.8388)	0.0007
8	1.1499	(1.1498, 1.1500)	0.0011
9	0.8387	(0.8386, 0.8388)	0.0007

anchored-ANOVA Collocation Surrogate

- Constructed surrogate using only first-order components.
- Required 123 evaluations of PARCS using Clenshaw-Curtis abscissas.
- Hierarchical surplus of 10^{-4} used to designate convergence.
- Surrogate sampled 500 times and multivariate distributions between assembly boxes calculated and compared to "true" solution.

Using anchored-ANOVA Collocation Surrogate to Reproduce Multivariate Distribution

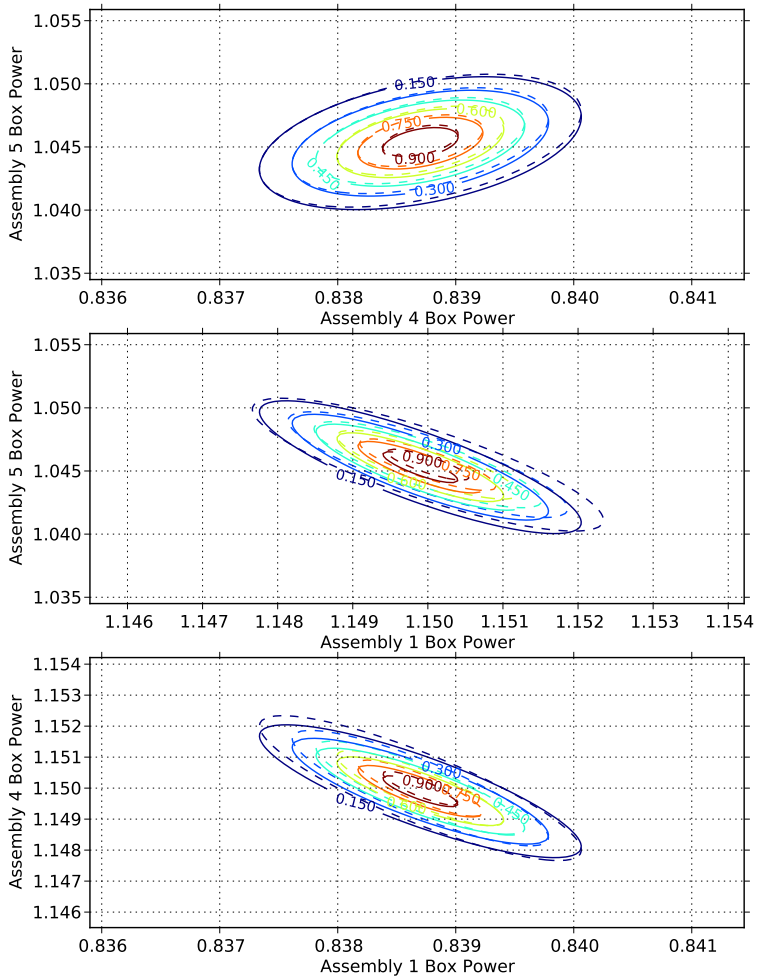

Outline

High Level Overview

- Fission reactions in UO_2 fuel generate the gases Xe and Kr in the fuel grains.
- Through a diffusive process these fission gases reach the grain face and begin to form bubbles.
- The bubbles increase in size as fission gases accumulate. Eventually, the bubbles coalesce and form multilobed pores.
- When bubbles come into contact with the grain edges gas is released from the grain faces.

Understanding Thermal FGR is Critical for Reactor Safety

- On one hand, if the Xe and Kr gases remain in the fuel matrix the fuel will swell.
- Potential result is clad damage or failure as contact pressure between fuel and clad increases.
- On the other hand, release of fission gases into rod free volume reduces the thermal conductivity of the fuel-clad gap and contributes to high operating pressures.
- Can result in clad lift-off and dangerous fuel temperature swings.

FGR in Pictures

Early Bubble Formations

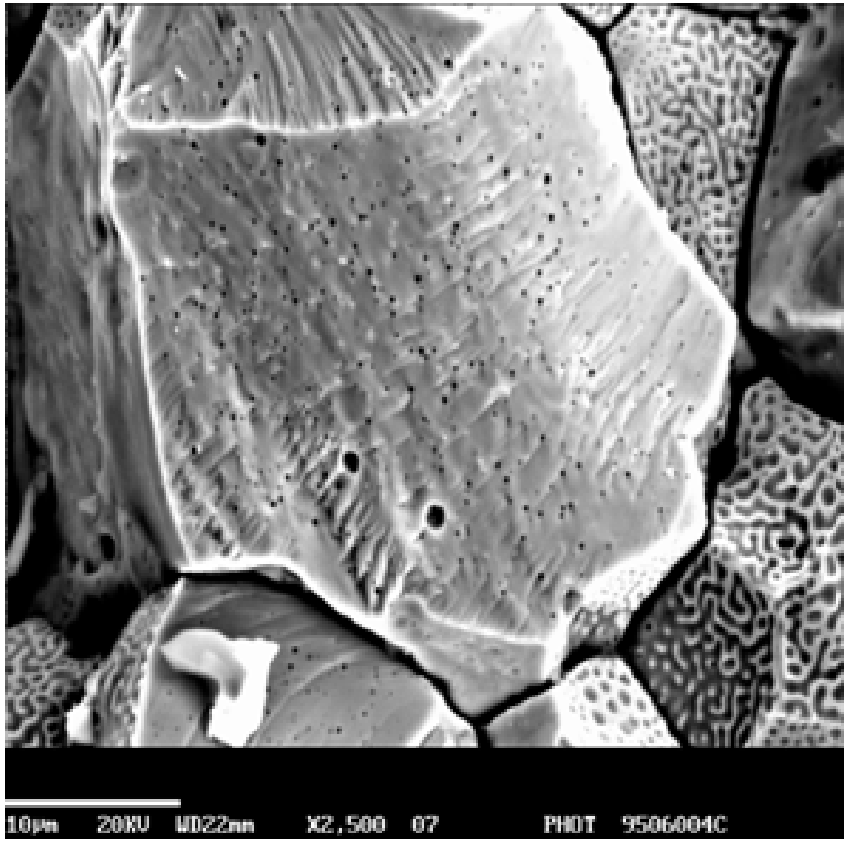

Bubble Coalescence

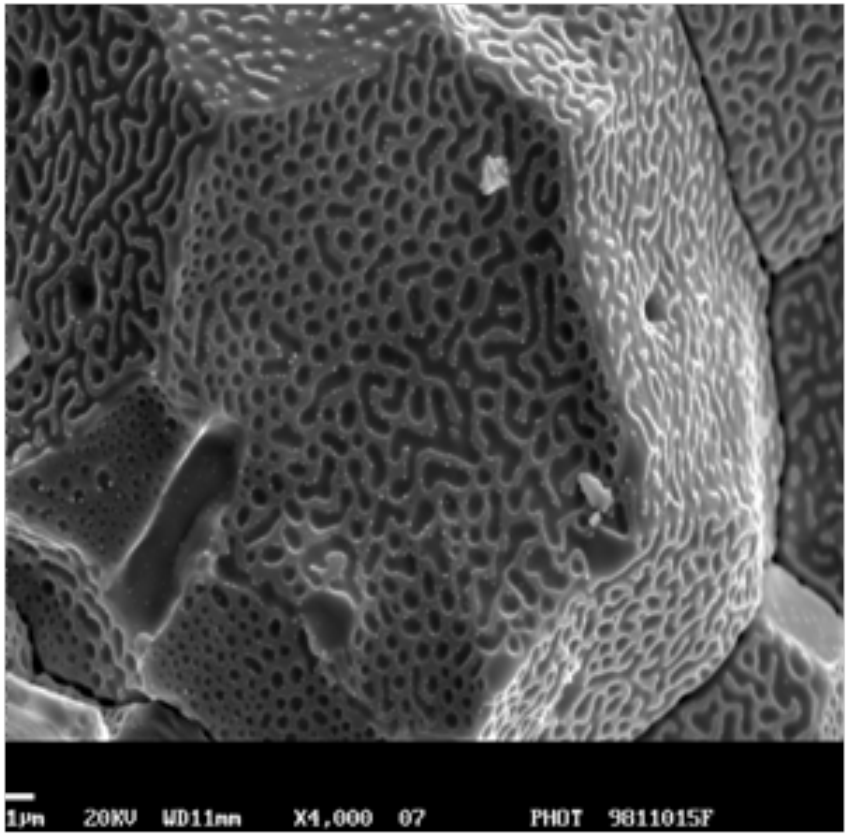

[1] G. Pastore, D. Pizzocri, J.D. Hales, S.R. Novascone, D.M. Perez, B.W. Spencer, R.L. Williamson, P. Van Uffelen, L. Luzzi, Modelling of Transient Fission Gas Behaviour in Oxide Fuel and Application to the BISON Code, Enlarged Halden Programme Group Meeting, Rros, Norway, September 7-12, 2014.

FGR in Pictures

Multi-lobed Pores

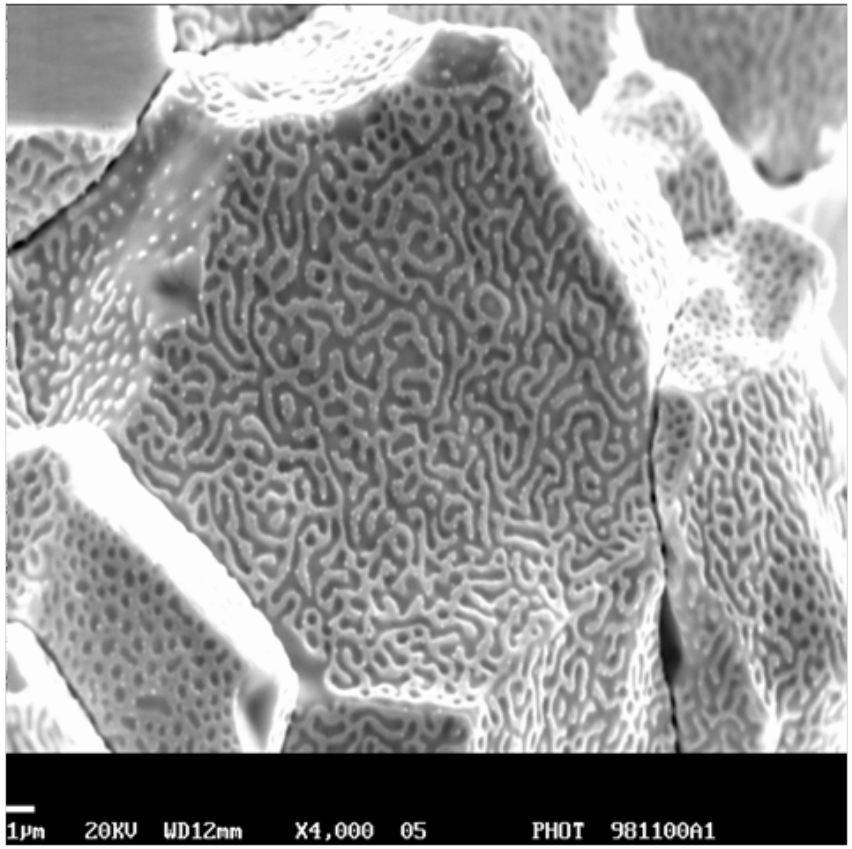

Gas Release

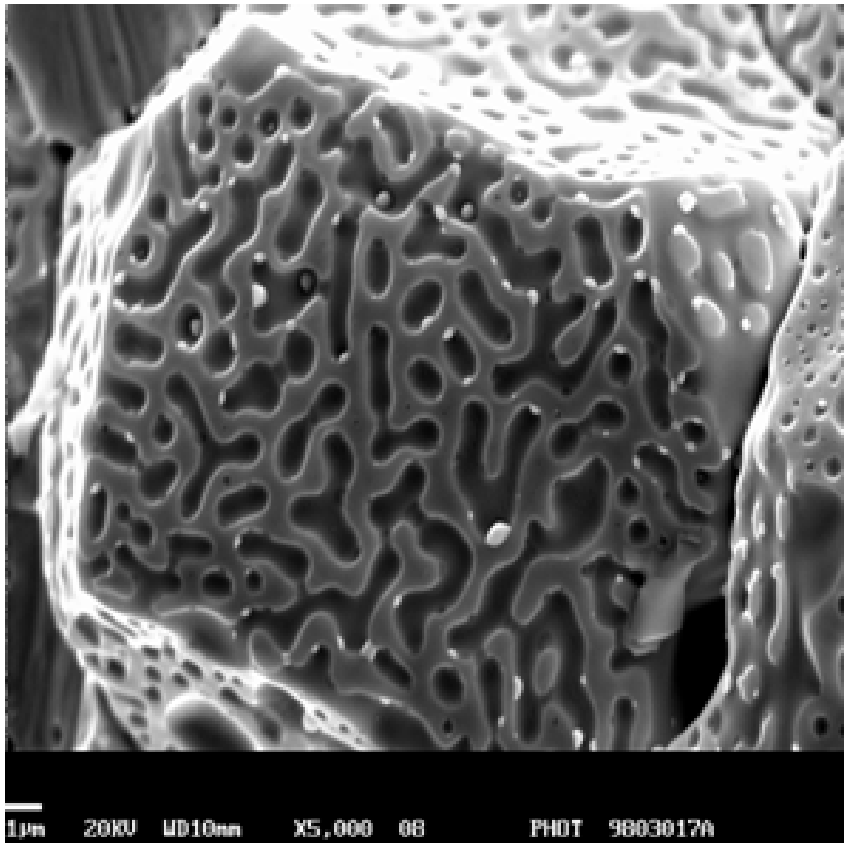

[1] G. Pastore, D. Pizzocri, J.D. Hales, S.R. Novascone, D.M. Perez, B.W. Spencer, R.L. Williamson, P. Van Uffelen, L. Luzzi, Modelling of Transient Fission Gas Behaviour in Oxide Fuel and Application to the BISON Code, Enlarged Halden Programme Group Meeting, Rros, Norway, September 7-12, 2014.

Modeling FGR: Intra-granular Gas Diffusion

- Describes how fission gases are transported from fuel grain to fuel face.
- The resolution parameter b describes the rate at which gas bubbles are destroyed due to irradiation and sent back into the fuel lattice.
- D_s is the single gas atom diffusion coefficient in a UO_2 lattice.

$$\frac{dC_{ig}}{dt} = \frac{b}{b+g} D_s \frac{1}{r^2} \frac{\partial}{\partial r} \left(r^2 \frac{\partial C_{ig}}{\partial r} \right) + \beta$$

Modeling FGR: Bubble Growth

- As gas atoms diffuse to the fuel grain boundary they get absorbed into bubble nuclei.
- The bubbles grow/shrink due to the absorption/emission of vacancies. Fission gas is mainly retained in the bubbles.

$$\frac{dV_{gf}}{dt} = \omega \frac{dn_g}{dt} + \Omega_{gf} \frac{dn_v}{dt}$$

Modeling FGR: Bubble Growth

$$\frac{dn_v}{dt} = \frac{2\pi D_v \delta_g}{kTs}(p - p_{eq})$$

- D_v is the vacancy diffusion coefficient, T is the fuel temperature.
- The pressure p_{eq} acting on the bubble is given as the difference between the bubble surface tension γ and the hydrostatic stress σ_h of the surrounding medium.
- Mechanical equilibrium requires that the pressure of the gas in the cavity be balanced by the bubble capillarity.

$$p_{eq} = \frac{2\gamma}{R_{gf}} - \sigma_h$$

Modeling FGR: Bubble Coalescence

- As the grain face bubbles begin to grow, they'll coalesce.
- Under the assumption of uniform bubble size and the conservation of total bubble volume, the relationship between the bubble number density N_{gf} and projected area on the grain face A_{gf} is:

$$\frac{dN_{gf}}{dt} = -\frac{6N_{gf}^2}{3 + 4n_{gf}A_{gf}}\frac{dA_{gf}}{dt}$$

Modeling FGR: Grain Face Saturation

- Thermal FGR occurs when the grain face saturation condition holds.

$$\frac{d\left(N_{gf}A_{gf}\right)}{dt} = 0$$

- The rate of thermal release is:

$$\frac{dC_{thr}}{dt} = \frac{3}{r_{gr}}\left(1 - P_f\right)\frac{d\psi_{thr}}{dt}$$

- The factors r_{gr} and P_f represent the fuel grain radius and fuel porosity, respectively.

Modeling FGR: Implementation

- The FGR model described here has been implemented and validated in the finite element-based fuel performance modeling code Bison by Pastore et. al.
- Bison is used to model the Risø AN3 FGR kinetics.
- Due to the relatively high temperatures involved in the Risø AN3 power ramp experiment athermal FGR is trumped by its thermal counterpart.
- Bison reports integral fission gas release values. Being a finite element code, Bison computes the gas release at each integration point.
- The ratio of total fission gas released into the rod free volume to the total fission gas generated at each integration point is the quantity of interest in this work.

FGR Parameters Used for Calibration

- Through a thorough literature review and discussions with Pastore et. al. the following parameters and uncertainty ranges are considered for calibration.

Description	Symbol	Lower Bound	Upper Bound	Scaled
Initial Fuel Grain Radius	$r_{g,0}$ $[m]$	2.0E-6	15.0E-6	no
Fuel Porosity	P_f	0.0	0.1	no
Surface Tension	γ $\left[J \cdot m^{-2}\right]$	0.5	1.0	no
Temperature	T	0.95	1.05	yes
Fuel Grain Radius	r_g	0.4	1.6	yes
Vacancy Diffusion Coef.	D_v $\left[m^2 \cdot s^{-1}\right]$	0.1	10.0	no
Resolution Parameter	b $\left[s^{-1}\right]$	0.1	10.0	no
Intra-granular Diffusion Coef.	D_s $\left[m^2 \cdot s^{-1}\right]$	0.316	3.162	no

Sampling FGR Parameters

- The FGR parameters are randomly sampled 100 times and propagated through Bison.

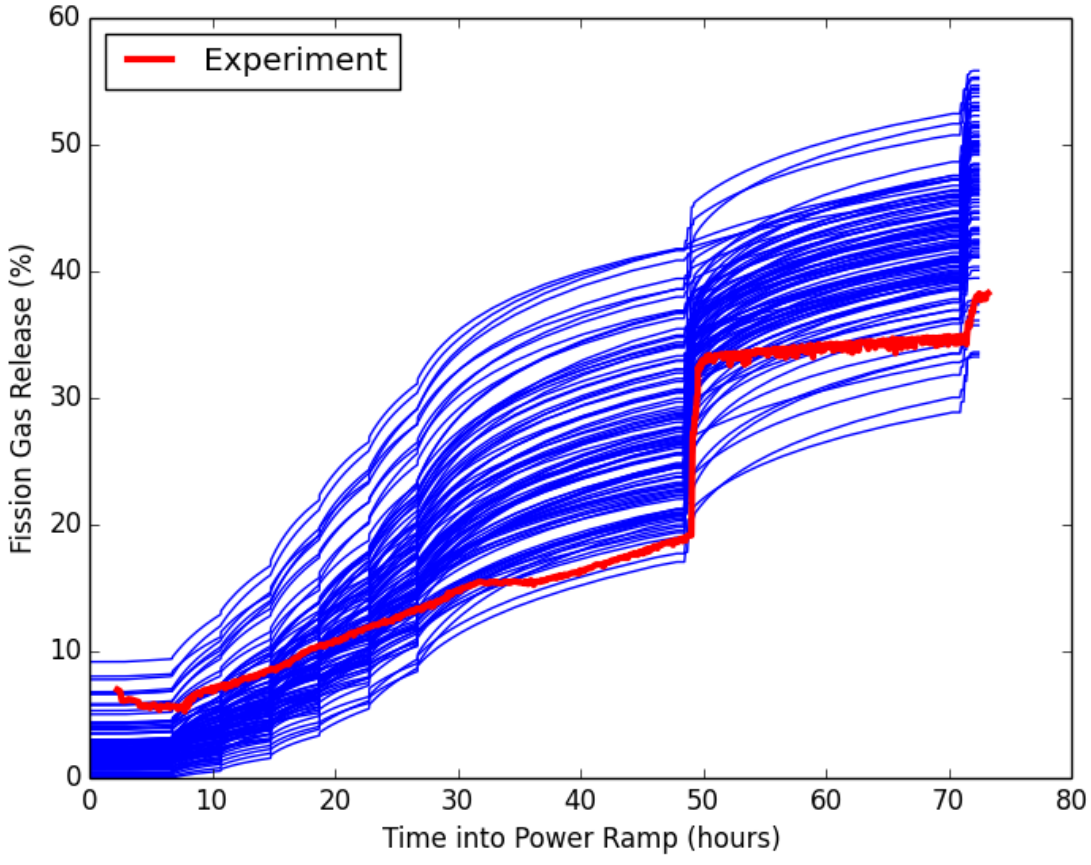

Modeling Problem

- Each FGR simulation in Bison takes approximately an hour using 16 processors.
- We need a fast mapping from the FGR parameters to FGR kinetics time series output by Bison for calibration.
- Surrogate methods described previously are really designed for acting on scalar quantities. We have a time series.
- Build a surrogate at each time-step? Inefficient. Unstable.
- Apply Principal Component Analysis (PCA) to model variations in FGR kinetics.

Applying PCA

Eigenvalues

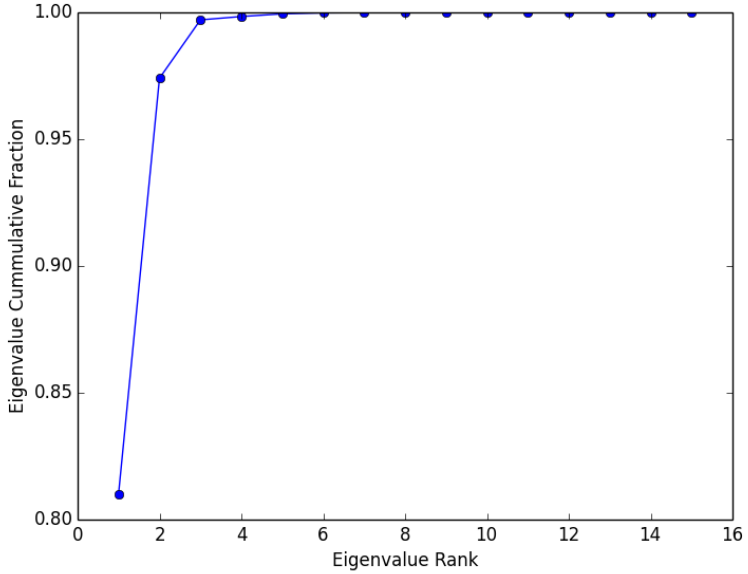

Top three eigenvectors

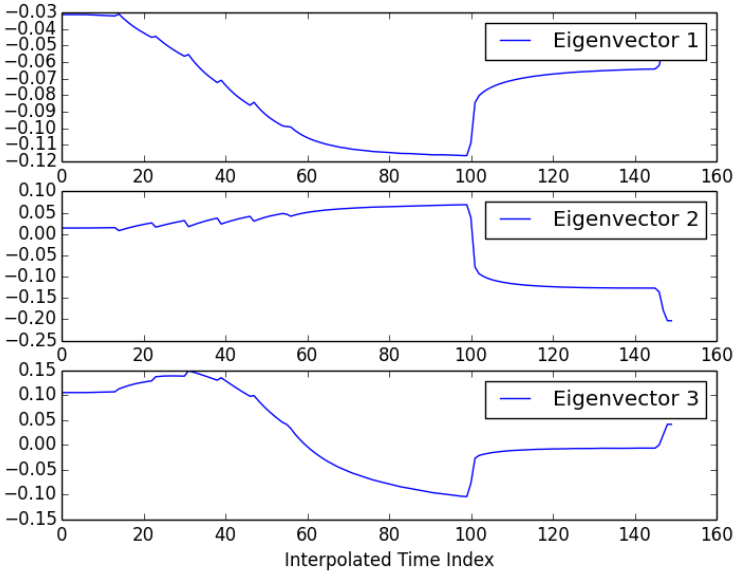

Insights with PCA

- The top three principal components account for over 99% of the variance in the simulated FGR kinetics.
- Correlate the variation in FGR parameter values with each of the principal components to see which parameters are the drivers of the variance.

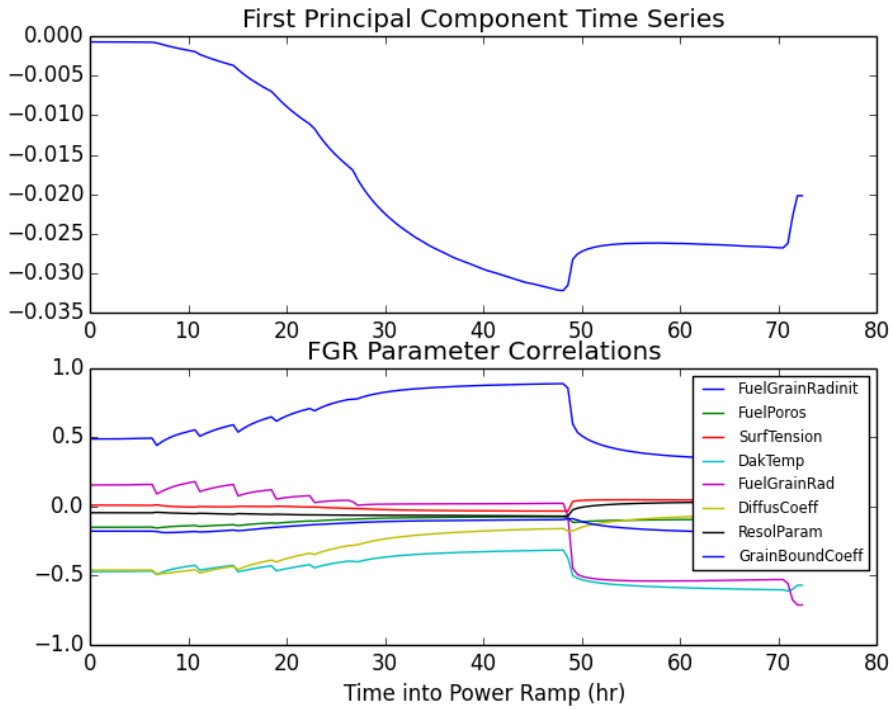

Using PCA for Surrogate Construction

- Through PCA we showed you can effectively represent any Bison FGR kinetics time series using three principal components.
- Use Kriging to construct three surrogates, each of which maps the FGR parameters R^i to one of the 3 PCA expansion coefficients $\hat{p}_{ij}$ corresponding to the principal components X_j for $j \in (1, 2, 3)$.

$$\hat{\mathcal{F}}^i(R^i) = \hat{p}_{i1}\left(R^i\right) X_1 + \hat{p}_{i2}\left(R^i\right) X_2 + \hat{p}_{i3}\left(R^i\right) X_3 + \mu$$

$$\sigma^2_{\hat{\mathcal{F}}^i} = \sigma^2_{\hat{p}_{i1}} X_1^2 + \sigma^2_{\hat{p}_{i2}} X_2^2 + \sigma^2_{\hat{p}_{i3}} X_3^2$$

Cross Validation

- 100 independent Bison simulations of the Risø AN3 power ramp are obtained (test set).
- PCA expansion coefficient surrogates are built on original 100 simulations (train set).
- Both inverse and logarithmic transforms are applied without increase in prediction accuracy.

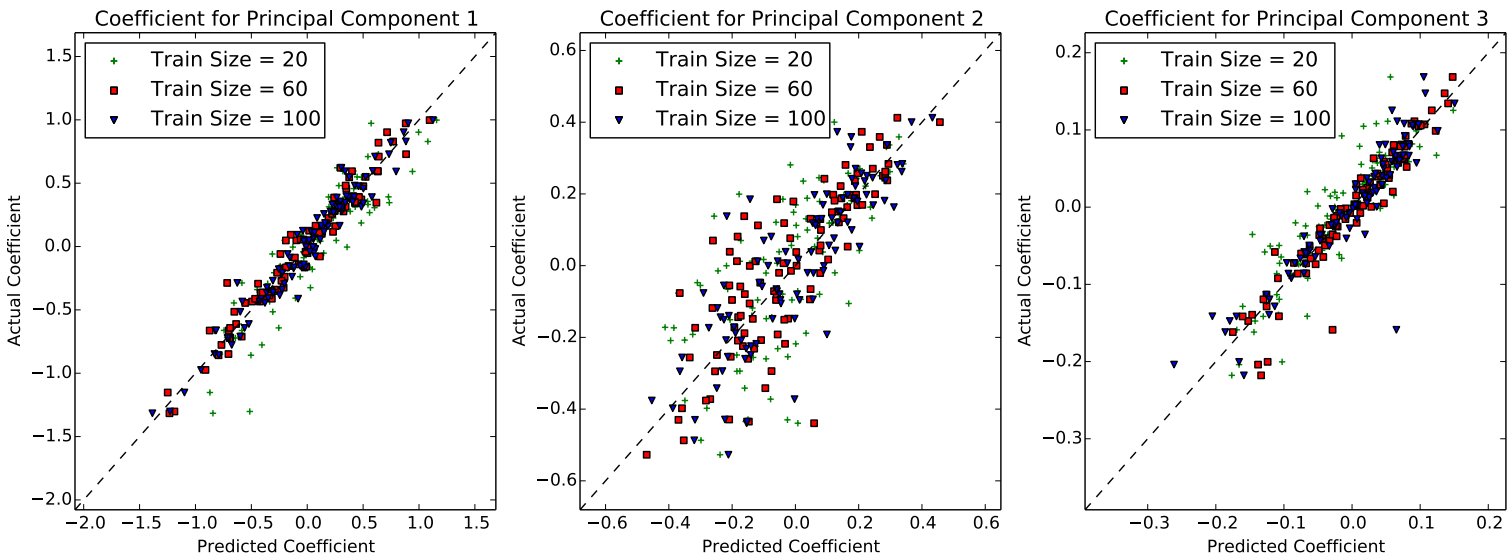

Cross Validation

- Standardized cross-validated residual plotted.

$$\frac{p_{ij} - \hat{p}_{ij}}{\sigma_{\hat{p}_{ij}}}$$

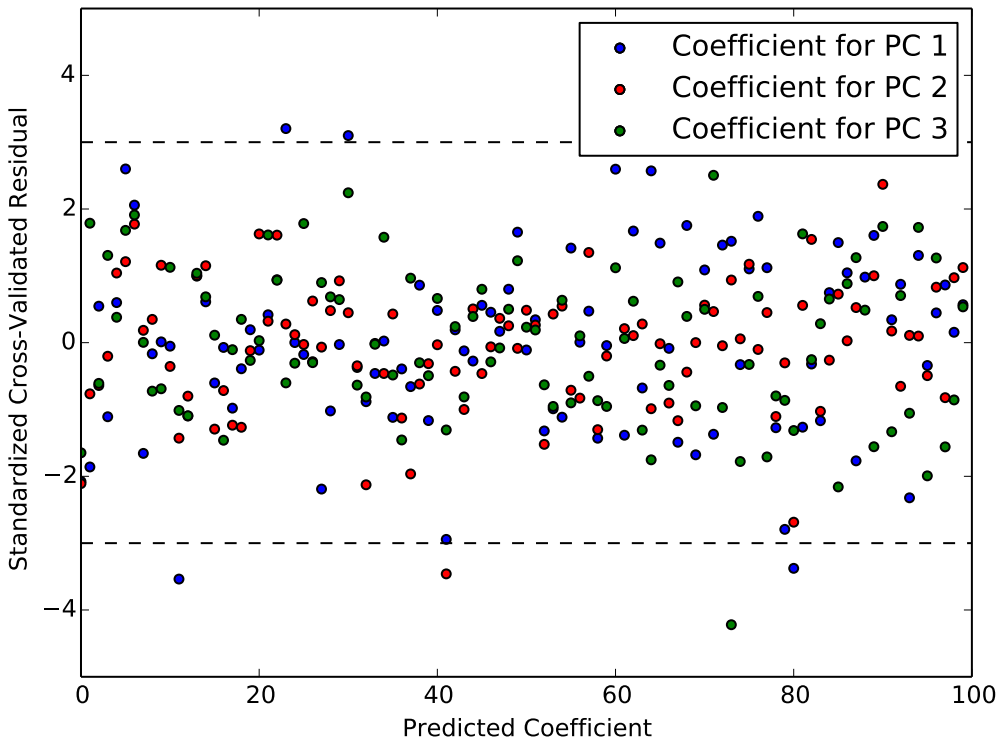

Calibration of FGR Parameters

- To determine the error between predicted time series the RMSE is used as a cost function.
- The objective of calibration is to find a set of fission gas release parameters such that the RMSE between prediction and experiment is minimized.
- Many potential algorithms to use for calibration (EGO, Nelder-Mead, COBYLA, Simplex, Newton-CG).
- To decide whether to use a global optimizer or local optimizer it's worthwhile to do some sensitivity analysis.

Sensitivity Analysis Using FGR Kinetics Surrogate

- Morris' Algorithm is initially applied to get a sense of which parameters interact with others and which have the largest main effects.
- A total of 4500 evaluations of the FGR kinetics surrogate are required to produce the plot below:

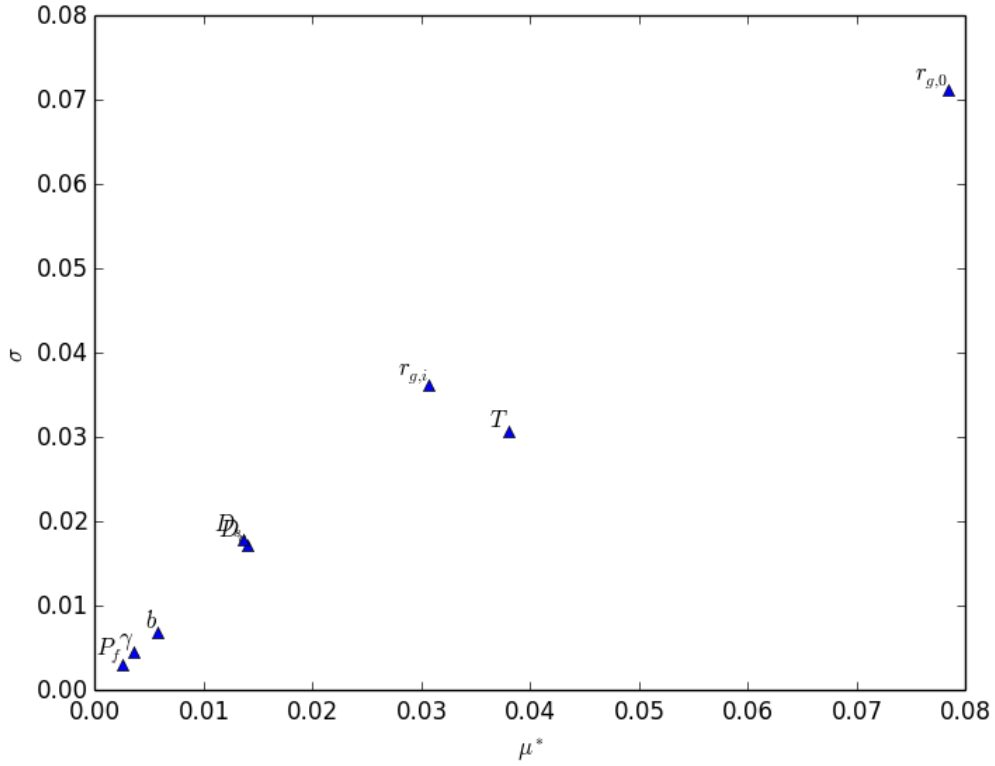

Sensitivity Analysis Using FGR Kinetics Surrogate

- Main and total effect indices for the RMSE using the Sobol-Jansen algorithm.
- A total of 10^5 instances of the surrogate are used to estimate the indices.

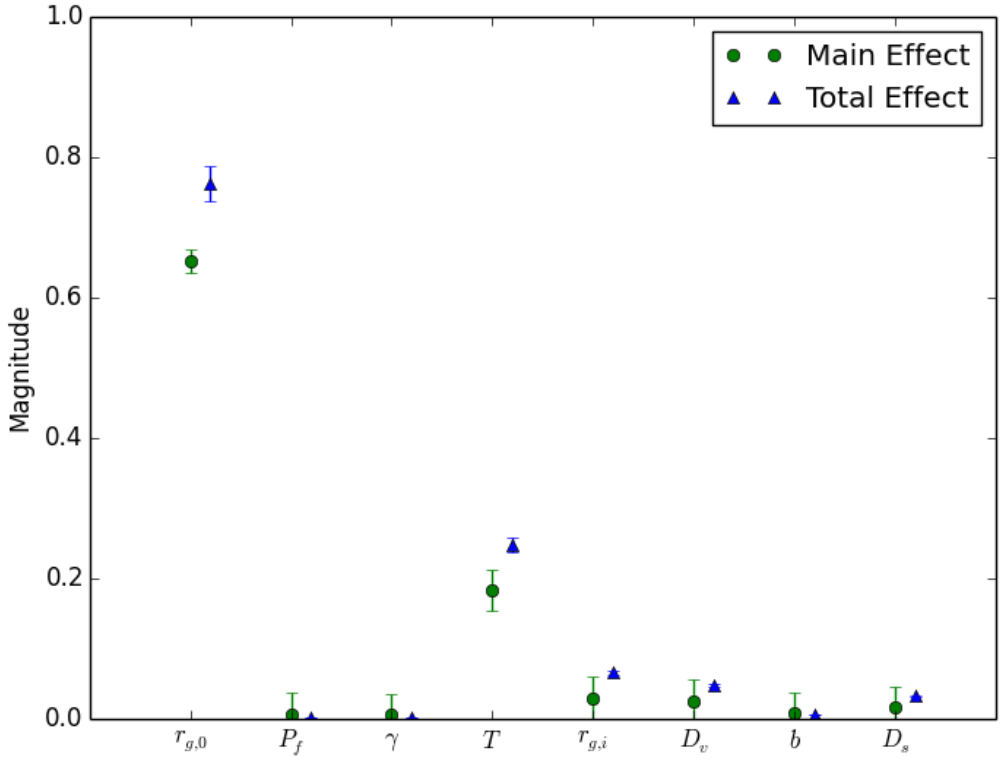

Sensitivity Analysis Using FGR Kinetics Surrogate

- Second order Sobol indices for the RMSE.
- A total of 3.7×10^5 instances of the surrogate are used to estimate the indices.

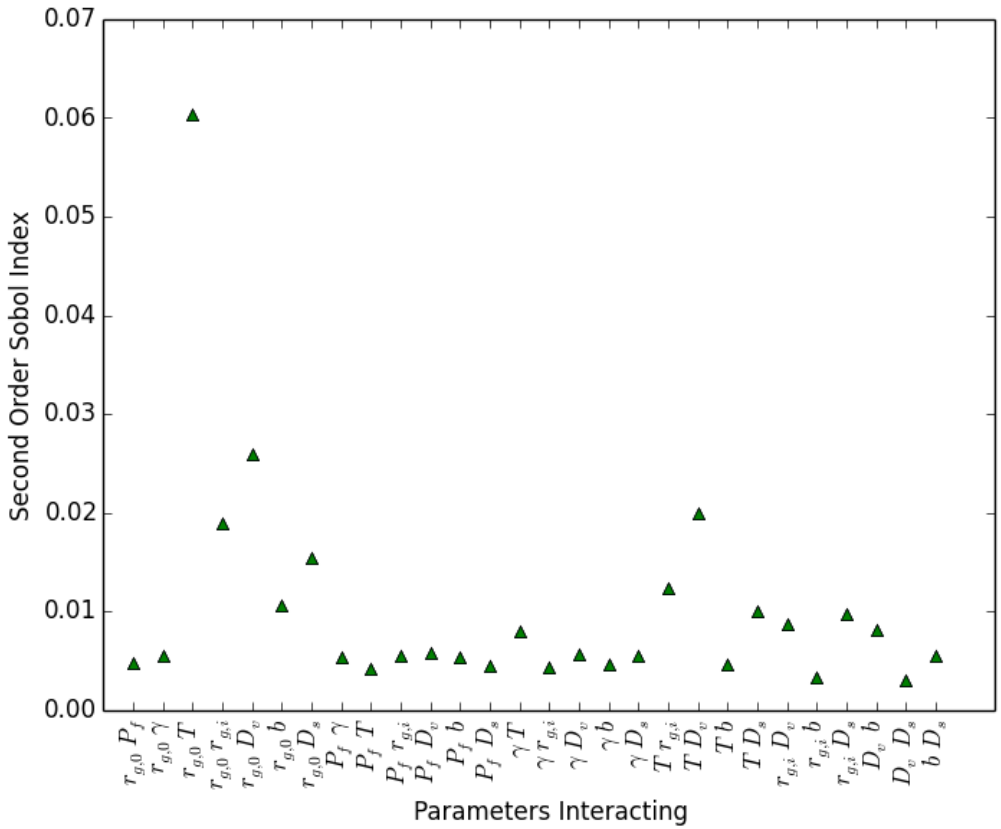

Calibrating the FGR Parameters

- Given the presence of strong interaction among the fission gas release parameters it is unlikely a global RMSE minimum can be found in reasonable time.
- A locally optimal solution can be found using the COBYLA algorithm.
- The COBYLA algorithm is of the simplex variety that does not require any gradient information while allowing for constraints to be placed on both the search parameters and objective function.
- For this problem it is necessary to not allow fission gas parameters that result in negative fission gas release values in predicted time series.

Calibrating the FGR Parameters

- Optimization algorithms such as COBYLA are sensitive to initial search conditions.
- The algorithm is executed 100 different times, with each execution being seeded by one of the 100 LHS used to construct the expansion coefficient surrogates.
- Such a procedure increases the probability of finding a true minimum RMSE and not one existing in a flat space.
- The minimum RMSE found was 2.94%.
- To identify the locally minimum RMSE some 10^5 instances of the surrogate were required.

Calibrating the FGR Parameters

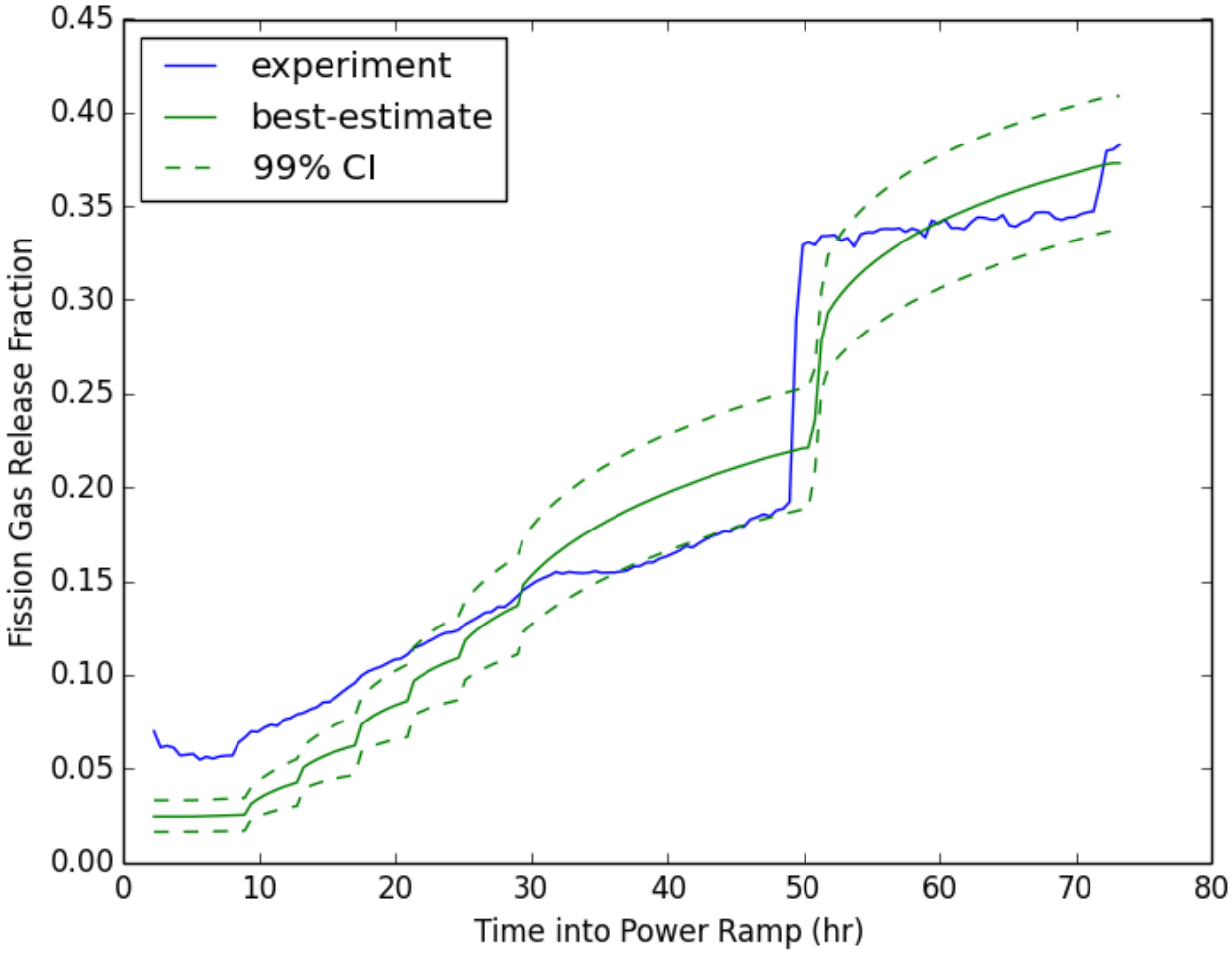

Calibrating the FGR Parameters

- Optimal parameter values, with each parameter scaled to the unit hypercube, found for each of the 100 COBYLA seedings is summarized in a boxplot.
- The length of the whiskers implies strong non-linear interaction effects.

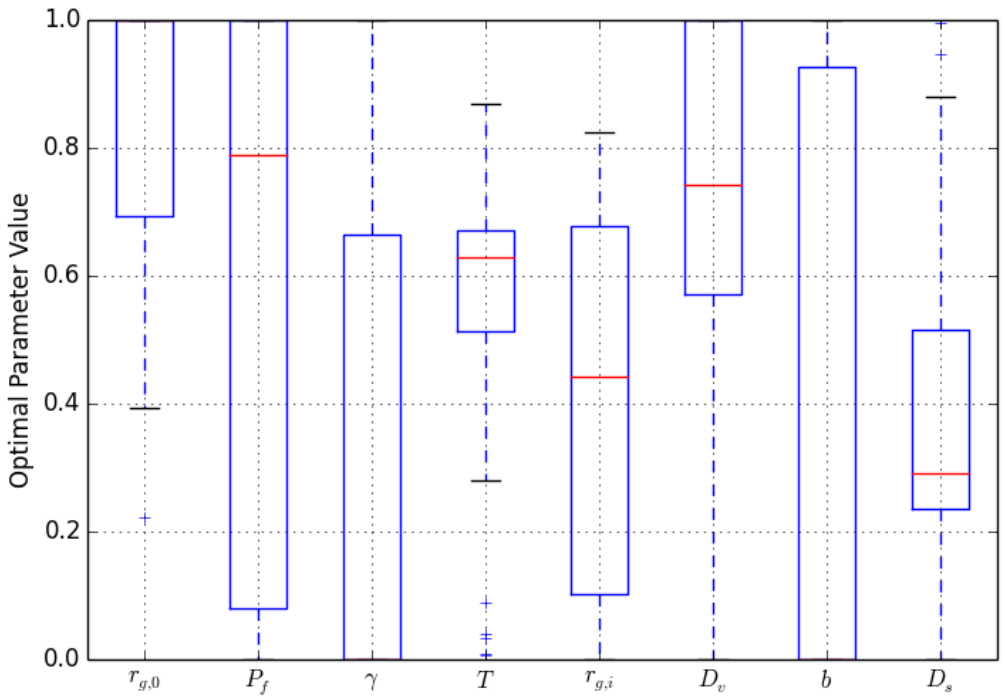

Smoothing Experimental Data

- At some points in the experimental data the total fission gas release decreases, which is not physical.
- However, with only a single time series measurement there is no way of assigning uncertainties to fission gas release values measured at different times throughout the power ramp.
- In an attempt to smooth the experimental data local polynomial regression was applied with the minimal amount of smoothing necessary to make the fission gas release time series strictly monotonically increasing.
- The locally minimal RMSE was calculated to be 2.49%, which is a 15.5% reduction in RMSE from when raw experimental data is utilized.

Smoothing Experimental Data

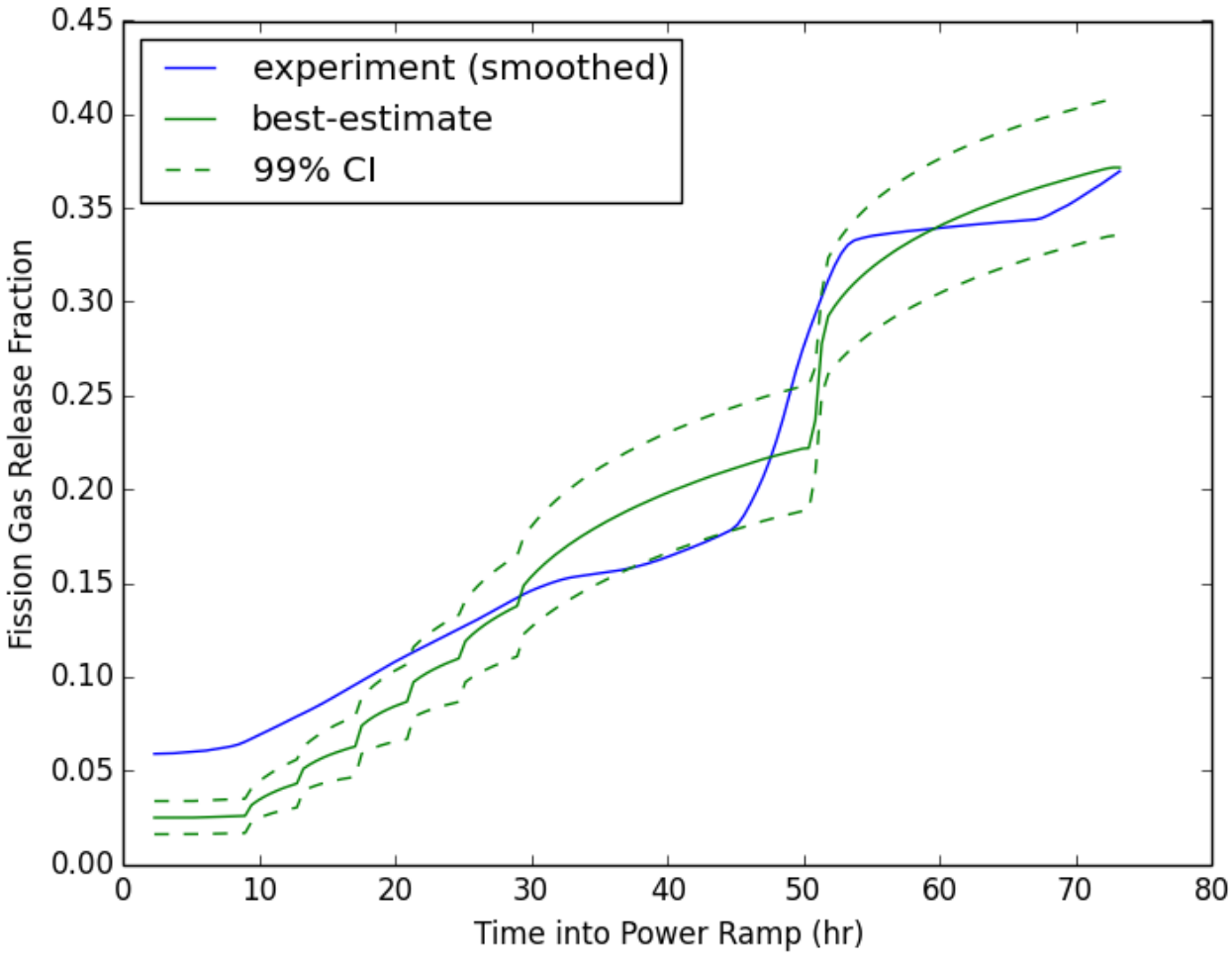

Outline

Summary of Calibration Results

- There are significant discrepancies between predicted and experimental time series, especially in the power burst occurring at hour fifty of the power ramp.
- For the case when raw experimental data is used there is only a 2.6% relative error in the EOE FGR prediction. The BOE prediction error is 64.8%.
- For the case of smoothed experimental date the prediction results are marginally improved with a BOE prediction error of 57.8% and an EOE error of 0.5%.
- It's possible to enforce the conditions of matching the predicted BOE and EOE predictions to their respective experimental values in the COBYLA framework.
- Enforcing only one of the conditions to a tolerance of 10^{-3} was achievable although the resulting solution grossly over predicted the fission gas release elsewhere in the time series.

Differences Between Prediction and Experiment

- There are apparent and irreconcilable differences between Bison's FGR predictions and the experimental data.
- Some of these differences can be attributed to several fission gas release aspects not explicitly modeled in Bison.
- Namely, burst fission gas release due to micro-cracking and the effect of measuring fission gas release using pressure transducers.
- Uncertainty in SIFGRS parameters not modeled in this research.

Insights From Sensitivity Analysis

- The fuel grain radius and fuel temperature had the highest sensitivity indices and produced the largest non-linear interaction effects with the other parameters.
- While sensitivity coefficients were calculated for the Risø AN3 problem, it is not certain that the same parameter conclusions would generalize to other fission gas kinetics problems.
- The same type of analysis as conducted here would likely have to be replicated for each unique problem.
- The lack of generalization is likely due to the unique profundity of physics in play for each type of problem.

Why Kriging?

- Non-linearity of fission gas release models coupled with large uncertainties implied the need for modeling higher-order interaction effects.
- Modeling such higher-order effects with anchored-ANOVA and Smolyak sparse grids can get very expensive, with no clear limit of how many objective function simulations will be needed.
- Transparency of Kriging appealing when considering each Bison fission gas release simulation would have to be performed in parallel.
- If simulations fail to converge or experiences an error, the correction process is straight forward. Contrarily, there are a lot of moving pieces in the anchored-ANOVA surrogate approach.
- Clear extension to time series.

Original Contributions of Research

- Construction of a surrogate model for the fuel performance code Bison and subsequent calibration of fission gas release parameters to experimental data from the FUMEX database.
- Extension of Kriging to construct surrogates for entire time series through PCA.
- Application of anchored-ANOVA decomposition and Smolyak sparse grids to construct surrogates for classic nuclear engineering problems.

Questions?

Sparse Grid Mechanics Example

- Consider a function of two dimensions $f(x_1, x_2)$, $d = 2$.
- Let's calculate the Level 1 (q=3) Smolyak sparse grid interpolant for f, $A_{3,2}(f)$.

$$\begin{aligned} A_{3,2}(f) &= A_{2,2}(f) + \Delta A_{3,2} \\ &= \Delta A_{2,2} + \cancel{A_{1,2}(f)} + \Delta A_{3,2} \end{aligned}$$

- First let's calculate $\Delta A_{2,2}$.

$$\Delta A_{2,2} = \sum_{|\mathbf{i}|=2} \left(f(x_{j_1}^{i_1}, x_{j_2}^{i_2}) - \cancel{A_{1,2}(f)(x_{j_1}^{i_1}, x_{j_2}^{i_2})} \right) \cdot \left(a_{j_1}^{i_1} \otimes a_{j_2}^{i_2} \right)$$

Sparse Grid Mechanics Example

- $|\mathbf{i}| = 2 \rightarrow i_1 + i_2 = 2 \rightarrow$ sum over the set of i indices $\{(1,1)\}$.
- Using Clenshaw-Curtis for $i = 1$ we have $m_i = 1$, namely the origin.

$$\Delta A_{2,2} = f\left(x_1^1, x_1^1\right) a_1^1 a_1^1$$

- In this case, $a_1^1 = 1$ and $x_1^1 = 0$ so $\Delta A_{2,2}$ amounts to evaluating the objective function at the hypercube origin.

Sparse Grid Mechanics Example

- Now let's calculate $\Delta A_{3,2}$.
- $|\mathbf{i}| = 3 \rightarrow i_1 + i_2 = 3 \rightarrow$ sum over the set of i indices $\{(1,2),(2,1)\}$.
- Using Clenshaw-Curtis for $i = 2$ we have $m_i = 3$ so $j \in \{1,2,3\}$

$$\begin{aligned}\Delta A_{3,2} &= \sum_{|\mathbf{i}|=3} \left(f(x_{j_1}^{i_1}, x_{j_2}^{i_2}) - A_{2,2}(f)(x_{j_1}^{i_1}, x_{j_2}^{i_2}) \right) \cdot \left(a_{j_1}^{i_1} \otimes a_{j_2}^{i_2} \right) \\ &= \sum_{|\mathbf{i}|=3} \left(f(x_{j_1}^{i_1}, x_{j_2}^{i_2}) - f\left(x_1^1, x_1^1\right) a_1^1 a_1^1 \right) \cdot \left(a_{j_1}^{i_1} \otimes a_{j_2}^{i_2} \right)\end{aligned}$$

Sparse Grid Mechanics Example

$$
\begin{aligned}
\Delta A_{3,2} = & \left[f(x_1^2, x_1^1) - f\left(x_1^1, x_1^1\right) a_1^1 a_1^1\right] a_1^2 a_1^1 \\
& + \left[f(x_2^2, x_1^1) - f\left(x_1^1, x_1^1\right) a_1^1 a_1^1\right] a_2^2 a_1^1 \\
& + \left[f(x_3^2, x_1^1) - f\left(x_1^1, x_1^1\right) a_1^1 a_1^1\right] a_3^2 a_1^1 \\
& + \left[f(x_1^1, x_1^2) - f\left(x_1^1, x_1^1\right) a_1^1 a_1^1\right] a_1^1 a_1^2 \\
& + \left[f(x_1^1, x_2^2) - f\left(x_1^1, x_1^1\right) a_1^1 a_1^1\right] a_1^1 a_2^2 \\
& + \left[f(x_1^1, x_3^2) - f\left(x_1^1, x_1^1\right) a_1^1 a_1^1\right] a_1^1 a_3^2
\end{aligned}
$$

- Due to the nestedness of Clenshaw-Curtis, points can be reused.
- For example, $f(x_1^1, x_1^1) = f(x_1^1, x_2^2) = f(x_2^2, x_1^1)$.

Sparse Grid Mechanics Example

- Putting everything together, the level 1 Sparse grid interpolant is:

$$
\begin{aligned}
A_{3,2}(f) &= \Delta A_{2,2} + \Delta A_{3,2} \\
&= f\left(x_1^1, x_1^1\right) a_1^1 a_1^1 \\
&+ \left[f(x_1^2, x_1^1) - f\left(x_1^1, x_1^1\right) a_1^1 a_1^1\right] a_1^2 a_1^1 \\
&+ \left[f(x_3^2, x_1^1) - f\left(x_1^1, x_1^1\right) a_1^1 a_1^1\right] a_3^2 a_1^1 \\
&+ \left[f(x_1^1, x_1^2) - f\left(x_1^1, x_1^1\right) a_1^1 a_1^1\right] a_1^1 a_1^2 \\
&+ \left[f(x_1^1, x_3^2) - f\left(x_1^1, x_1^1\right) a_1^1 a_1^1\right] a_1^1 a_3^2
\end{aligned}
$$